# Part V

# Boundary Processes

# Chapter 14

# Sea surface fluxes

The governing equations introduced in Chapter 2 need boundary conditions. At the sea surface, they take the form of the flux boundary condition. Momentum fluxes for the equations of motion, heat and material fluxes for the temperature and other tracer equations, and fresh water fluxes for the continuity equation. These surface fluxes are the main driving force of oceanic motions. This chapter explains how they are treated in MRI.COM.

Ideally, the realistic momentum, heat and fresh water fluxes based on observation should be used when a realistic simulation is intended. However, because existing sea surface fluxes derived from observations include large errors and the ocean models have their own errors, it is not common for an ocean-sea ice model in stand-alone mode to be driven by fluxes without a feedback process. It is a common practice for an ocean-sea ice model to compute fluxes using a bulk formula with sea surface meteorological elements derived from atmospheric reanalysis data and the surface temperature and velocity of its own.

Section 14.1 describes momentum flux. How heat fluxes are treated is described in Sections 14.2 through 14.5. Treatment of fresh water fluxes is described in Section 14.6, including the computations of the equivalent fluxes under invariable first layer volume condition (Section 14.6.2). Sections 14.7 and 14.8 explain how heat and fresh water fluxes are used in temperature and salinity equations. Several options are available for the choice of the bulk formula to calculate momentum, latent and sensible heat, and evaporative fluxes. They are detailed in Section 14.9 along with a general formulation for bulk transfer coefficients. How to give the attributes of external forcing data to the model is explained in Section 14.10. Finally, some technical details are presented in Sections 14.11 and 14.12.

Here is a cautionary note. Although recent satellite observations enable us to obtain sea surface fluxes with high resolution in space and time, even higher accuracy is necessary for practical uses. For example, a bias of several $\mathrm{W\,m^{-2}}$ in heat flux may greatly affect the thickness of sea ice, meaning that accuracy on the order of several $\mathrm{W\,m^{-2}}$ is necessary to clarify climatic change (WGASF, 2000). Efforts in enhancing observations and evaluating sea surface fluxes based on various methods have been expanded globally. In the future, a high-resolution ocean model and a new scheme for advection and diffusion may be developed to improve the simulation capability. It is noted, however, that increased observation frequency does not necessarily guarantee improved accuracy of the fluxes (for example, it is unlikely that the accuracy of a bulk coefficient would be improved). Hence, it should be kept in mind that sea surface fluxes presently involve large uncertainties.

## 14.1 Momentum flux (surface stress)

### 14.1.1 Formulation

Surface forcing to the momentum equation, or surface momentum flux into the ocean, is in the form of wind stress (or stress from sea ice), and is treated as a body force to the first level velocity in the model algorithm

$$\frac{\partial}{\partial t}(u_1, v_1) = \ldots + \frac{(\tau_x, \tau_y)}{\rho_0 \Delta z_{\frac{1}{2}}}, \tag{14.1}$$

where $(u_1, v_1)$ is horizontal velocity at the first level, $\Delta z_{\frac{1}{2}}$ is the thickness of the first layer, $\rho_0$ is the reference density of sea water (Table 2.1), and $\tau_x$ and $\tau_y$ are zonal and meridional stresses.

Surface stress is an area weighted average of stresses due to surface wind and sea ice:

$$(\tau_x, \tau_y) = (1 - A)(\tau_{AO_x}, \tau_{AO_y}) + A(\tau_{IO_x}, \tau_{IO_y}), \tag{14.2}$$

where $A$ is the area fraction of sea ice. $\overrightarrow{\tau_{AO}}$ and $\overrightarrow{\tau_{IO}}$ are air-ocean and ice-ocean stresses, respectively.

Wind stress (air-sea momentum flux) vector, $\overrightarrow{\tau_{AO}}$ is computed by using the wind vector of the surface air, $\overrightarrow{U_a}$, the first

level velocity (surface current), $\overrightarrow{U_s}$, and a bulk transfer coefficient $C_D$ (see Section 14.9 for computation) as follows:

$$\overrightarrow{\tau_{AO}} = \rho_a C_D |\overrightarrow{U_a} - \alpha\overrightarrow{U_s}|(\overrightarrow{U_a} - \alpha\overrightarrow{U_s}), \tag{14.3}$$

where $\rho_a$ is the density of air and $\alpha$ is the contribution of the surface current to the calculation of relative surface wind. Usually, $\alpha$ is unity, but it can be tuned to reduce damping effect of the wind stress on the oceanic current (see Table 14.3).

See Chapter 17 for the computation of ice-ocean stress ($\overrightarrow{\tau_{IO}}$).

### 14.1.2 Numerical implementation

On implementing Eq. (14.3), the time level of the surface velocity must be the starting time level of the integration. Because the corrector substep is the main body of the LFAM3 time integration scheme (Section 4.3), we use the n-th step surface velocity at the starting time level of the corrector substep.

$$\overrightarrow{\tau_{AO}}^n = \rho_a C_D |\overrightarrow{U_a}^n - \alpha\overrightarrow{U_s}^n|(\overrightarrow{U_a}^n - \alpha\overrightarrow{U_s}^n). \tag{14.4}$$

The same treatment should be applied to the computation of ice-ocean stress. Note that surface fluxes including the momentum flux are calculated in the predictor substep and the same fluxes are reused in the corrector substep.

In the bulk formulae implemented in MRI.COM, bulk transfer coefficients are computed on the tracer point. Those on the velocity point are obtained as area-weighted averages from the surrounding tracer points.

### 14.1.3 Usage

#### a. Model option

By default, wind stress vector is given as external data and each component should be read from separate files. (Wind stress data is always required, and thus files filled with zeros are necessary when wind stress is not applied.) The input data should be in units of [dyn cm$^{-2}$]. When `TAUBULK` option is specified, the wind stress is calculated by using a bulk formula. In this option, components of wind vector at 10 m in units of [cm s$^{-1}$] should be prepared as external data, instead of the default wind stress data.

#### b. Input data

Time series of wind stress or surface wind vector data on a structured lattice should be prepared in the single precision, direct access format with a constant time interval. The data may be interpolated in time and space in the model. Attributes of the data are specified by `nml_force_data`. The name of the data and the units assumed by the model are listed on Table 14.1. The name of the data should be "U-wind" and "V-wind" regardless of wind stress or wind vector. See Section 14.10 for details on how to specify external forcing files.

Table14.1 Wind data to be read from namelist `nml_force_data`.

| | name | units | usage |
|---|---|---|---|
| X-ward wind stress | U-wind | dyn cm$^{-2}$ | if not `TAUBULK` |
| Y-ward wind stress | V-wind | dyn cm$^{-2}$ | if not `TAUBULK` |
| X-ward wind speed | U-wind | cm s$^{-1}$ | if `TAUBULK` |
| Y-ward wind speed | V-wind | cm s$^{-1}$ | if `TAUBULK` |

#### c. Namelist

At the initial stage of the model integration, wind stress or wind may be gradually set up from zero at the start and unity after a specified period. The set up period is specified in namelist `nml_force_windsetup` (Table 14.2).

Table14.2 Namelist `nml_force_windsetup`.

| variable name | units | description | usage |
|---|---|---|---|
| `idays_wind_setup` | day | wind set up period in days | default : no tapering on wind |

Contribution of the surface current to the calculation of relative surface wind in (14.3) may be tuned by namelist `nml_bulk_wind` (Table 14.3). This is because the use of full surface current may lead to too strong damping on swift surface current in some model settings.

Table14.3 Namelist `nml_bulk_wind`.

| variable name | units | description | usage |
|---|---|---|---|
| `current_contri_factor` | 1 | Contribution of the surface current to the calculation of relative surface wind | default = 1.0 |

## 14.2 Heat flux

### 14.2.1 Formulation

There are four main components in surface heat flux: shortwave radiation ($Q_{SH}$), longwave radiation ($Q_{LO}$), latent ($Q_{LA}$), and sensible ($Q_{SN}$) heat flux. Specific expression for these fluxes is shown in the following sections. In addition to those fluxes, the heat exchanges with the sea ice ($Q_{\mathrm{ice}}$) and the heat transport due to surface fresh water fluxes ($F^{\theta}_{WF}$) contribute to surface heat flux. See Section 14.6 for fresh water fluxes and Chapter 17 for details of exchange with sea ice.

The total sea surface heat flux $Q_{NET}$ is given by

$$Q_{NET} = Q_{SH} + Q_{LO} + Q_{LA} + Q_{SN} + Q_{\mathrm{ice}} + \rho_0 c_p F^{\theta}_{WF}, \tag{14.5}$$

where $\rho_0$ and $c_p$ are density and specific heat of sea water. Note that downward heat flux is defined as positive.

### 14.2.2 Numerical implementation

The components of net heat flux (14.5) are broken into three terms,

$$Q_{NET} = Q_{SH} + Q_{OTHER} + \rho_0 c_p F^{\theta}_{WF}. \tag{14.6}$$

Shortwave radiation ($Q_{SH}$) penetrates into the ocean interior. Other terms ($Q_{OTHER}$) are absorbed in the first layer. Fresh water transport term ($\rho_0 c_p F^{\theta}_{WF}$) needs separate treatment because it should be consistent with the continuity equation and included in the solution procedures of the tracer advection term.

### 14.2.3 Usage

#### a. Model options

The `HFLUX` option must be selected to treat surface heat fluxes explicitly in the model.

#### b. Input data

Time series of shortwave and longwave radiation, surface air temperature, surface specific humidity, surface wind speed, and sea-level pressure on a structured lattice should be prepared. The data may be interpolated in time and space in the model. Attributes of the data are specified by `nml_force_data`. The name of the data and the units assumed by the model are listed on Table 14.4. See Section 14.10 for details on how to specify external forcing files at run time.

Table14.4 Heat flux data to be read from namelist `nml_force_data` when `HFLUX` option is selected.

| elements | name | units | usage |
|---|---|---|---|
| Downward shortwave radiation | ShortWave | erg $s^{-1}$ $cm^{-2}$ = $\times 10^{-3}$ W $m^{-2}$ | |
| Downward longwave radiation | LongWave | erg $s^{-1}$ $cm^{-2}$ | |
| Surface air temperature | TempAir | °C | |
| Surface air specific humidity | SphAir | 1 | |
| Scalar wind speed | ScalarWind | cm $s^{-1}$ | unnecessary if `TAUBULK` |
| Sea level pressure | SeaLevelPressure | hPa | also used for `SLP` |

## 14.3 Shortwave radiation flux

### 14.3.1 Formulation

By default, the downward shortwave radiation ($Q_{SH}^{\mathrm{down}}$) is read as external forcing data. A part of the downward shortwave radiation ($\alpha_o Q_{SH}^{\mathrm{down}}$) is reflected at the sea surface, and the remainder penetrates into the ocean interior as the net shortwave radiation flux ($Q_{SH}(z=\eta) = (1-\alpha_o)Q_{SH}^{\mathrm{down}}$), where $\alpha_o$ is the albedo at the sea surface and $\eta$ is the position of sea surface in the fixed vertical coordinate. More than 50% of the radiation (in the near infra-red band) is absorbed within a depth of 1 m below the sea surface, but the remainder (in the visible and ultraviolet bands) penetrates further into the ocean interior and affects the subsurface temperature structure.

The penetrating shortwave radiation is expressed as a function of depth ($z$) in a fixed frame $Q_{SH}(z)$ and its vertical convergence $\partial Q_{SH}(z)/\partial z$ warms the sea water.

$$\frac{\partial \theta}{\partial t} = \ldots + \frac{1}{\rho_0 c_p}\frac{\partial Q_{SH}(z)}{\partial z}, \tag{14.7}$$

where $\rho_0$ is the density of sea water and $c_p$ is the specific heat of sea water. There are three options regarding how the vertical profile of shortwave penetration is specified.

#### a. Standard scheme of penetration

According to Paulson and Simpson (1977), the shortwave radiation flux penetrating into the ocean interior is given by using the fraction of the near infra-red band ($R$) and the attenuation distances for the near infra-red band ($\zeta_1$) and the visible and ultraviolet band ($\zeta_2$) as,

$$Q_{SH}(z) = Q_{SH}(0)[R\exp\{(-\eta+z)/\zeta_1\} + (1-R)\exp\{(-\eta+z)/\zeta_2\}], \tag{14.8}$$

where we set $R = 0.58$, $\zeta_1 = 35\,\mathrm{cm}$, and $\zeta_2 = 2300\,\mathrm{cm}$, using the optical properties of Water Type I based on the classification by Jerlov (1976). $Q_{SH}(0)$ is the net solar radiation flux at the sea surface.

#### b. A penetration scheme that takes into consideration of the insolation angle

The `SOLARANGLE` option enables us to include the effect of the insolation angle on the shortwave radiation flux in the oceanic interior. This scheme is based on Ishizaki and Yamanaka (2010). In this case, if the depth ($z$) on the r.h.s. of Equation (14.8) is replaced by the penetrating distance from the sea surface, the shortwave radiation is given by

$$Q_{SH}(z) = Q_{SH}(0)[R\exp\{(-\eta+z)/(\zeta_1\sin\theta_w)\} + (1-R)\exp\{(-\eta+z)/(\zeta_2\sin\theta_w)\}], \tag{14.9}$$

where $\theta_w$ is the penetrating angle in the ocean interior. When `SOLARANGLE` option is specified in coupled models, Equation (14.9) is replaced by

$$Q_{SH}(z) = Q_{SH_b}(z) + Q_{SH_d}(z), \tag{14.10}$$

where $Q_{SH_b}(z)$ and $Q_{SH_d}(z)$ are the shortwave radiation fluxes due to direct (beam) and diffuse solar radiation. Those fluxes are expressed as follows:

$$Q_{SH_b}(z) = Q_{SH_b}(0)[R_b\exp\{(-\eta+z)/(\zeta_1\sin\theta_w)\} + (1-R_b)\exp\{(-\eta+z)/(\zeta_2\sin\theta_w)\}], \tag{14.11}$$

$$Q_{SH_d}(z) = Q_{SH_d}(0)[R_d\exp\{(-\eta+z)/\zeta_1\} + (1-R_d)\exp\{(-\eta+z)/\zeta_2\}], \tag{14.12}$$

where $R_b$ and $R_d$ are the ratios of near infra-red to total radiation in direct (beam) and diffuse solar radiation, respectively. $Q_{SH_b}(0)$ and $Q_{SH_d}(0)$ are the net direct (beam) and diffuse solar radiation fluxes at the sea surface.

#### c. A penetration scheme that takes into consideration of chlorophyll concentration

Recent studies indicate that solar radiation absorption and local heating within the upper ocean are strongly influenced by the chlorophyll concentration. By specifying `CHLMA94` and `NPZD` options, we can use a shortwave penetration model with the chlorophyll concentration (Morel and Antoine, 1994). In this scheme, the shortwave radiation flux penetrating into the ocean interior is given by

$$Q_{SH}(z) = Q_{SH}(0)[R\exp\{(-\eta+z)/\zeta_0\} + (1-R)(V_1\exp\{(-\eta+z)/\zeta_1\} + V_2\exp\{(-\eta+z)/\zeta_2\})]. \tag{14.13}$$

The first exponential is for the infra-red waveband (> 750 nm), which is not influenced by biological materials and attenuates with a distance of $\zeta_0 = 26.7$ cm. The second and third exponentials are for the visible and ultraviolet bands (< 750 nm). $V_1$, $V_2$, $\zeta_1$, and $\zeta_2$ are calculated from an empirical relationship as a function of chlorophyll concentration ($chl$ [mg $\cdot$ m$^{-3}$]) as follows:

$$V_1 = 0.321 + 0.008C + 0.132C^2 + 0.038C^3 - 0.017C^4 - 0.007C^5, \tag{14.14}$$

$$V_2 = 0.679 - 0.008C - 0.132C^2 - 0.038C^3 + 0.017C^4 + 0.007C^5, \tag{14.15}$$

$$\zeta_1 = 1.540 - 0.197C + 0.166C^2 - 0.252C^3 - 0.055C^4 + 0.042C^5, \tag{14.16}$$

$$\zeta_2 = 7.925 - 6.644C + 3.662C^2 - 1.815C^3 - 0.218C^4 + 0.502C^5, \tag{14.17}$$

where $C = \log_{10}(chl)$. It is noted that $V_1 + V_2 = 1$.

When `SOLARANGLE` option is added to the options mentioned above, the shortwave radiation is slightly modified by

$$\begin{aligned} Q_{SH}(z) = & Q_{SH}(0)[R\exp\{(-\eta + z)/(\zeta_0 \sin\theta_w)\} \\ & + (1-R)(V_1\exp\{(-\eta + z)/(\zeta_1 \sin\theta_w)\} + V_2\exp\{(-\eta + z)/(\zeta_2 \sin\theta_w)\})]. \end{aligned} \tag{14.18}$$

In coupled models, Equation (14.18) is replaced by

$$Q_{SH}(z) = Q_{SH_b}(z) + Q_{SH_d}(z), \tag{14.19}$$

where $Q_{SH_b}(z)$ and $Q_{SH_d}(z)$ are the shortwave radiation fluxes due to direct (beam) and diffuse solar radiation. These fluxes are expressed as follows:

$$\begin{aligned} Q_{SH_b}(z) = & Q_{SH_b}(0)[R_b\exp\{(-\eta + z)/(\zeta_0 \sin\theta_w)\} \\ & + (1-R_b)(V_1\exp\{(-\eta + z)/(\zeta_1 \sin\theta_w)\} + V_2\exp\{(-\eta + z)/(\zeta_2 \sin\theta_w)\})], \end{aligned} \tag{14.20}$$

$$\begin{aligned} Q_{SH_d}(z) = & Q_{SH_d}(0)[R_d\exp\{(-\eta + z)/\zeta_0\} \\ & + (1-R_d)(V_1\exp\{(-\eta + z)/\zeta_1\} + V_2\exp\{(-\eta + z)/\zeta_2\})], \end{aligned} \tag{14.21}$$

where $R_b$ and $R_d$ are the ratios of near infra-red to total radiation for direct (beam) and diffuse solar radiation, respectively.

#### d. Albedo schemes

There are five options for the sea surface albedo. The first option is a constant value, which should be specified as `alb` in namelist `nml_albedo_ocean`.

The second option is based on Large and Yeager (2009) and is given by

$$\alpha_o = 0.069 - 0.011\cos(2\phi), \tag{14.22}$$

where $\phi$ is latitude.

The third option is based on Barker and Li (1995) and is given by

$$\alpha_o = 0.06 + 0.0421x^2 + 0.128x^3 - 0.04x^4 + \left(\frac{3.12}{5.68+U} + \frac{0.074x}{1.0+3.0U}\right)x^5, \tag{14.23}$$

where $x = 1 - \sin\theta_a$ ($\theta_a$ is a height angle of the Sun), and $U$ is the surface wind speed [m s$^{-1}$].

The fourth option is based on Briegleb et al. (1986) and is given by

$$\alpha_o = \frac{0.026}{(\sin\theta_a)^{1.7} + 0.065} + 0.15\,(\sin\theta_a - 0.1)\,(\sin\theta_a - 0.5)\,(\sin\theta_a - 1.0)\,. \tag{14.24}$$

The fifth option is based on Taylor et al. (1996) and is given by

$$\alpha_0 = \frac{0.037}{1.1\,(\sin\theta_a)^{1.4} + 0.15}. \tag{14.25}$$

### 14.3.2 Numerical implementation

Shortwave flux is computed on T-cells, which means that variations of horizontal cross section due to topography ($S$) must be taken into account. The vertical profile of the shortwave penetration can be expressed as a function of the vertical depth from the sea surface. Discrete form of the absorption of shortwave heat for a grid cell $(i, j, k - \frac{1}{2})$ is

$$(\theta V)^{n+1}_{i,j,k-\frac{1}{2}} = (\theta V)^{n}_{i,j,k-\frac{1}{2}} + \ldots + \Delta t\left(Q^n_{SHi,j,k-1}S_{i,j,k-\frac{1}{2}} - Q^n_{SHi,j,k}S_{i,j,k+\frac{1}{2}}\right). \tag{14.26}$$

### 14.3.3 Usage

a. Model option

- SOLARANGLE must be selected to take the solar penetration angle into consideration
- CHLMA94 must be selected to take the effect of chlorophyll concentration into consideration. The chlorophyll concentration will be taken from either the biogeochemical model with NPZD option or climatology (name = ChlorophyllClimatology) with CHLCLIM option.

When CHLCLIM option is selected, time series of 2-D chlorophyll concentration should be prepared. The data may be interpolated in time and space in the model. See Section 14.10 for how to specify external forcing files.

b. Namelist

Namelists related to shortwave radiation are listed on Tables 14.5 through 14.7.

Table14.5 Namelist nml_albedo_ocean.

| variable name | units | description | usage |
|---|---|---|---|
| alb | no (real8) | constant albedo | |
| albedo_scheme_name | no (character) | name of albedo scheme | 'constant' or 'const' : constant given by alb (default)<br>'CORE' or 'Large and Yeager 2009' : Large and Yeager (2009)<br>'MRI-ESM1', 'Barker and Li 1995' or 'Barker95' : Barker and Li (1995)<br>'Briegleb et al 1986' or 'Briegleb86' : Briegleb et al. (1986)<br>'Taylor et al 1996' or 'Taylor96' : Taylor et al. (1996) |
| albedo_choice | no (integer) | choice of albedo scheme (obsolete) | 1 : constant given by alb<br>2 : Large and Yeager (2009)<br>3 : Barker and Li (1995) |

Table14.6 Namelist nml_solarangle.

| variable name | units | description | usage |
|---|---|---|---|
| interval_shortwave_sec | sec | time interval of shortwave data | required |
| l_variable_zenith_ang | logical | use zenith angle with daily variation | default = .true. |
| l_const_zenith_ang_mean | logical | use average zenith angle from sunrise to sunset | valid if l_variable_zenith_ang = .false. |
| l_const_zenith_ang_noon | logical | use zenith angle at noon | valid if l_variable_zenith_ang = .false. |
| l_diurnal_var_shortwave | logical | daily variational amplitude of solar flux is calculated in this module | default = .false., If this is true, interval_shortwave_sec = 86400 |
| l_penetr_ang_considered | logical | introduction of transmitted angle based on Snell's law | default = .true. |

Table14.7 Namelist nml_frac_nearir.

| variable name | units | description | usage |
|---|---|---|---|
| qsratio_nearIR | no (real8) | ratio of near infra-red band to the total shortwave flux ($R$) | default = 0.58 |

## 14.4 Longwave radiation flux

### 14.4.1 Formulation

Net longwave radiation into the ocean $Q_{LO}^{\text{net}}$ is the residual between the downward longwave radiation $Q_{LO}^{\text{down}}$ (external data given by user) and the upward black body radiation of sea water with the sea surface temperature ($\theta_{\text{surf}}$),

$$Q_{LO}^{\text{net}} = (1 - r)Q_{LO}^{\text{down}} - e_m \sigma (\theta_{\text{surf}} + 273.15)^4. \tag{14.27}$$

Here, $e_m$ is the emissivity for sea water, which should be specified by user, $r$ is the reflectance of longwave radiation, and $\sigma = 5.67 \times 10^{-5}$ erg $\cdot$ s$^{-1}$ $\cdot$ cm$^{-2}$ $\cdot$ K$^{-4}$ is the Stefan-Boltzmann constant. The longwave reflectance is calculated as $r = 1 - a - t$, where $a$ and $t$ are the absorbance and the transmittance, respectively. Assuming that $a = e_m$ from the Kirchhoff's law and $t = 0$, we give the reflectance $r$ by $1 - e_m$.

### 14.4.2 Numerical implementation

There is no special issue on the numerical implementation. The net longwave flux is absorbed in the first layer of the model. Before used to update the first level temperature, it is summed into an array (`qothr`) which gathers all heat flux components except for shortwave. Note that the sea surface (first model level) temperature at the starting time level is used to evaluate upward longwave flux in any time integration scheme.

### 14.4.3 Usage

a. Namelist

Emissivity ($e_m$) of black body radiation from the sea surface may be specified by user at run time with namelist `nml_emissivity_sea_water` (Table 14.8).

Table14.8 Namelist `nml_emissivity_sea_water`.

| variable name | units | description | usage |
|---|---|---|---|
| `emissivity` | no (real8) | emissivity of upward longwave radiation from sea water | default = 1.0 |

## 14.5 Latent and sensible heat fluxes

### 14.5.1 Formulation

The bulk method is used to calculate latent and sensible heat fluxes. In the bulk method, latent heat flux ($Q_{LA}$) and sensible heat flux ($Q_{SN}$) are calculated using bulk transfer coefficients $C_E$ and $C_H$ (see Section 14.9),

$$Q_{LA} = -\rho_a L C_E |\Delta \vec{U}| (q_s - q_a), \tag{14.28}$$

$$Q_{SN} = -\rho_a c_{pa} C_H |\Delta \vec{U}| (T_s - \theta_a). \tag{14.29}$$

Here, $\rho_a$ is the air density, $L$ is the latent heat of evaporation, $q_a$ is the specific humidity of the surface air, $q_s$ is the saturated specific humidity of the sea surface temperature, $\theta_a$ is the surface air potential temperature (K), $T_s$ is the absolute sea surface water temperature (K), and $\Delta \vec{U} = \vec{U}_a - \alpha \vec{U}_s$ is the vector difference between the surface wind and the first level velocity (surface current). As explained in relation to the wind stress (Section 14.1), $\alpha$ is the contribution of the surface current to the calculation of the relative wind vector. The quantity $c_{pa}$ is the specific heat of air.

### 14.5.2 Numerical implementation

There is no special issue on the numerical implementation. The latent and sensible heat fluxes are absorbed in the first layer of the model. Before used to update the first level temperature, they are summed into an array (`qothr`) which gathers all heat flux components except for shortwave. Note that the sea surface (first model level) temperature at the starting time level is used to evaluate fluxes in any time integration scheme.

### 14.5.3 Usage

Model option

MRI.COM can provide two calculation methods for bulk transfer coefficients. One of them must be specified when `HFLUX` option is chosen.

- `BULKNCAR` for Large and Yeager (2004; 2009)
- `BULKECMWF` for ECMWF (2016b)

See Sections 14.9.2 and 14.9.3 for details.

## 14.6 Freshwater flux

### 14.6.1 Formulation

Freshwater flux through the sea surface ($F^W$) is caused mainly by precipitation ($P$), evaporation ($E$), river discharge ($R$), and formation-melting of sea ice ($I$):

$$F^W = P - E + R + I, \tag{14.30}$$

Precipitation and river discharge are given as input data. MRI.COM conventionally considers precipitation on the sea as rainfall and precipitation on sea ice as snowfall. It is possible to separately specify rainfall data and snowfall data ($P = P_{\rm rain} + P_{\rm snow}$; Table 14.9). Note that rainfall on the sea ice in this case passes through the sea ice and falls directly on the sea. Fresh water flux due to sea ice formation-melting is given by the sea ice model. Evaporation is computed by a bulk formula in the ocean model and it should be consistent with the latent heat flux:

$$E = \rho_a C_E |\Delta\vec{U}|(q_s - q_a) = -Q_{LA}/L. \tag{14.31}$$

Note that evaporation ($E$) is defined as positive upward.

Fresh water flux is treated as the surface boundary condition for the surface height equation:

$$\frac{\partial \eta}{\partial t} = \ldots + F^W. \tag{14.32}$$

Fresh water is added to/subtracted from the surface grid cell. Thickness of grid cells in the whole vertical column should be modified to adapt to this change in the surface height. Concentration of materials (tracer species) in a grid cell should be updated by taking into account of these volume changes. Knowledge about the contents of materials in the fresh water flux is required for the computation, which is explained below.

### 14.6.2 Material fluxes due to fresh water flux

Rainfall, evaporation, and river discharge ($P_{\rm rain} - E + R$) are assumed to have the first level temperature ($\theta_{\rm surf}$) and zero salinity. We assume that the snow temperature is 0°C and its salinity is 0. Melting heat of snowfall is supplied from the top layer of the ocean model. In addition, fresh water flux is simply added to the first layer volume. Thus, the downward temperature and salinity transports to the first layer due to the fresh water flux are given as follows:

$$F^\theta_{WF} = (P_{\rm rain} - E + R) \cdot \theta_{\rm surf} + F^\theta_I - F^\theta_{\rm SnowMelt}, \tag{14.33}$$

$$F^S_{WF} = F^S_I. \tag{14.34}$$

where $F^\theta_I$ and $F^S_I$ are temperature and salinity transport due to the water exchange between the ocean and sea ice, respectively. Those fluxes are calculated in the sea ice model (Eqs. (17.252) and (17.255)). The salinity transport is induced only by the water exchange between the ocean and sea ice, and other water inflows are assumed to have zero salinity. These downward transports of temperature and salinity are treated as downward vertical advection terms at the top of the first ocean model layer (Eqs. (14.36) and (14.39) ).

### 14.6.3 Numerical implementation

a. Suppressing long-term drift of sea water volume

Because the global mean of $F^W$ should not necessarily be zero and there is no feedback mechanism in an ocean-sea ice system to balance the fresh water budget, the globally averaged volume of the ocean may continue to increase or decrease.

To avoid this, the integral of the globally averaged freshwater flux is set to zero by selecting `WADJ` option,

$$F^W_{ADJ} = F^W - \overline{F^W}, \tag{14.35}$$

where $\overline{F^W}$ is the global mean of $F^W$ ($= P - E + R$), where $E$ includes sublimation over sea ice. Note that exchange with sea ice is not included in the computation of $\overline{F^W}$.

### 14.6.4 Usage

#### a. Model options

- `WFLUX` should be specified to explicitly treat fresh water fluxes in the model. In this case, precipitation data must be prepared as input data.
- `RUNOFF` enables river discharge to be treated. River run-off data should be given as external data.
- `WADJ` imposes conservation of sea water volume of the ocean - sea ice system.

#### b. Input data

When `WFLUX` and `RUNOFF` options are specified, time series of precipitation and river run-off data must be prepared, respectively. Users can use namelist `nml_force_snowfall` (Table 14.9) to control whether snowfall data is read individually or not. The freshwater flux read from "Precipitation" data is regarded as rainfall if the users explicitly specify the snowfall data. Data on a structured lattice should be prepared in the single precision direct access format with a constant time interval. Attributes of the data are specified by `nml_force_data`. Name and units assumed by the model are summarized in Table 14.10.

The data may be interpolated in time and space in the model. See Section 14.10 for how to specify external forcing files.

Table14.9 Namelist `nml_force_snowfall`.

| variable name | units | description | usage |
|---|---|---|---|
| `l_read_snowfall` | logical | Read snowfall data in addition to precipitation (rainfall) data | default = `.false.` |

Table14.10 Water flux data to be read from namelist `nml_force_data`.

| element | name | units | usage |
|---|---|---|---|
| precipitation | Precipitation | g s$^{-1}$ cm$^{-2}$ | `WFLUX` |
| river discharge | RiverDischargeRate | g s$^{-1}$ cm$^{-2}$ | `RUNOFF` |
| snowfall | Snowfall | g s$^{-1}$ cm$^{-2}$ | `WFLUX`; required when `l_read_snowfall` = `.true.` (Table 14.9) |

#### c. Namelist

The river run-off data around Antarctica may be treated as the discharge of iceberg if sea ice is present in the grid. Namelist `nml_mkflux` specifies this behavior (Table 14.11).

Table14.11 Namelist `nml_mkflux`. See also Table 14.13.

| variable name | units | description | usage |
|---|---|---|---|
| `l_glacier` | logical | if a rivermouth grid has sea ice then river discharge is converted into iceberg input from glacier | default = `.false.` |

Continued on next page

Table 14.11 – continued from previous page

| variable name | units | description | usage |
|---|---|---|---|
| `l_after_rivermouth_spread` | logical | river discharge is converted into iceberg after a smoothing operation of river discharge data | default = .`false`. |

When `WADJ` option is selected, the global summation of surface fresh water fluxes, which is used for determining the offsetting flux, can be made MPI parallel independent by choosing `l_strict_waterflux_adjust` = .`true`. in namelist `nml_waterflux_adjust` (Table 14.12).

Table14.12 Namelist `nml_waterflux_adjust`.

| variable name | units | description | usage |
|---|---|---|---|
| `l_strict_waterflux_adjust` | logical | water flux adjustment is made MPI parallel independent | default = .`false`. |

## 14.7 Treatment in the temperature equation

### 14.7.1 Formulation

The contributions of surface forcing ($F_z^\theta$), shortwave radiation flux ($Q_{SH}$) and the heat transport due to fresh water flux (14.33, $F_{WF}^\theta$) to the first layer temperature are expressed as

$$\left.\frac{\partial\theta}{\partial t}\right|_{k=\frac{1}{2}} = \ldots + \frac{F_z^\theta \Delta A}{\Delta V} + \frac{1}{\rho_0 c_p}\frac{\partial Q_{SH}}{\partial z} + \frac{F_{WF}^\theta \Delta A}{\Delta V}, \tag{14.36}$$

where $\Delta A$ and $\Delta V$ are the horizontal area and the volume of the first layer of a T-cell, respectively. The term ($F_z^\theta$) consists of the net sea surface heat flux except for the shortwave radiation flux ($Q_{OTHER}$), restoring of SST ($\theta_{\rm surf}$) to a specified value ($\theta^*$), and heating associated with freezing of supercooled water $\theta_t^{\rm supercool}$ :

$$\frac{F_z^\theta \Delta A}{\Delta V} = \frac{Q_{OTHER}\Delta A}{\rho_0 c_p \Delta V} - \frac{\overline{\Delta z}_{\frac{1}{2}}}{\gamma_\theta}\frac{(\theta_{\rm surf}-\theta^*)\Delta A}{\Delta V} + \theta_t^{\rm supercool}. \tag{14.37}$$

The heat flux ($Q_{OTHER}$) has been converted to temperature transport using the reference density ($\rho_0$) and specific heat ($c_p$) of sea water. The second term on the r.h.s. is a restoring term to a specified SST. The parameter $\gamma_\theta$ is a restoring time (in units of seconds) and should be read from input file (see Chapter 13). The restoring term is converted to temperature transport by multiplying the (fixed) thickness of the first layer of a T-cell ($\overline{\Delta z}_{\frac{1}{2}}$).

By default, surface temperature forcing consists only of the restoring term. By specifying `HFLUX` option, sea surface heat fluxes are treated explicitly. The heat transport due to fresh water flux are included when `WFLUX` option is specified.

### 14.7.2 Numerical Implementation

The heat transport due to fresh water flux ($F_{WF}^\theta$ in 14.36) is incorporated in the advection schemes. Shortwave absorption is treated separately from other heat flux terms. Heat flux components except for the shortwave radiation are gathered in an array (`qothr`) and added to the tendency of the first layer temperature.

Heating of supercooled water ($\theta_t^{\rm supercool}$) is calculated as follows:

$$\theta_t^{\rm supercool} = -\frac{1}{\Delta t}(\theta_{\rm surf}-\theta_{\rm freeze}) \qquad \text{if} \quad \theta_{\rm surf} < \theta_{\rm freeze}. \tag{14.38}$$

When the temperature of the first layer is below the freezing point, the temperature is set to the freezing point and this heat comes from the latent heat release of the new sea ice formation. This is done in the sea ice model. Because the sea ice part uses the forward scheme to proceed in time, the sea surface temperature at the "current" time level must be given to the sea ice part from the ocean part. The result is that the temperature below the freezing point at the "current" time level is modified and adjusted to the freezing point by the sea ice part. This treatment is not compatible with the leap-frog time stepping employed by the ocean part. Specifically, treating this temperature adjustment process in a form of heat flux exchange may result in a numerical instability. Though the modification of sea surface temperature in the sea ice part is inconvenient for some purposes, we keep this treatment until a revision of time-stepping scheme is considered. (That is,

the sea water temperature is directly corrected in the sea ice model, and its heating tendency is calculated in the ocean model afterward.) See Sec. 17.2.3 for sea ice formation by freezing of supercooled water in the sea ice model.

## 14.8 Treatment in the salinity equation

The fresh water flux ($F_W$) modifies the volume but not the salt content of the surface layer, changing the salinity of the surface layer (see also Chapter 7). Since fresh water flux is not related directly to the sea surface salinity, the model sea surface salinity might be far from the observed value. Hence, an adjustment is sometimes needed to restore the model sea surface salinity to the observed one (see the last term on the r.h.s. of the next equation). Generally, the model salinity is restored to the observed climatological sea surface salinity since no reliable data set of historical sea surface salinity is available at present.

### 14.8.1 Formulation

The contributions of explicit surface forcing ($F_z^S$) and the salt transport due to formation and melting of sea ice (14.34, $F_{WF}^S$) to the first layer salinity are expressed as

$$\left.\frac{\partial S}{\partial t}\right|_{k=\frac{1}{2}} = \ldots + \frac{F_z^S \Delta A}{\Delta V} + \frac{F_{WF}^S \Delta A}{\Delta V}, \tag{14.39}$$

where $\Delta V, \Delta A$ are the same as those in (14.36).

The explicit surface forcing ($F_z^S$) consists of restoring of SSS ($S_{\rm surf}$) to a specified value ($S^*$) and salinity correction by the sea ice model $S_t^{\rm ice}$:

$$\frac{F_z^S \Delta A}{\Delta V} = -\frac{\overline{\Delta z}_{\frac{1}{2}}}{\gamma_s} \frac{(S_{\rm surf} - S^*)\Delta A}{\Delta V} + S_t^{\rm ice}. \tag{14.40}$$

The parameter $1/\gamma_s$ is a reciprocal of a restoring time (in units of seconds) and should be read from input file (see Chapter 13). The restoring term is converted to salinity transport by multiplying $\overline{\Delta z}_{\frac{1}{2}}$, as in (14.37). Users have a variety of options for SSS restoring (see Table 14.14).

The salinity correction by the sea ice model $S_t^{\rm ice}$ is calculated as follows:

$$S_t^{\rm ice} = \frac{1}{\Delta t}(S_{\rm ice} - S_{\rm surf}) - \frac{F_{IO}^S \Delta A}{\Delta V}, \tag{14.41}$$

where $S_{\rm surf}$ is SSS at the current time step, $S_{\rm ice}$ is the modified SSS in the sea ice model, and $F_{IO}^S$ is a salinity flux between ocean and sea ice without the water exchange [cm psu $s^{-1}$] (positive upward) (Eq. 17.95). $S_t^{\rm ice} = 0$ in an ocean only model without a sea ice model.

### 14.8.2 Numerical Implementation

The salinity transport due to fresh water flux is incorporated in the advection schemes. The first layer salinity is calculated by taking into consideration of the volume change of the grid cell due to the continuity equation.

### 14.8.3 Usage

a. Model option

- `WFLUX` treats fresh water fluxes explicitly in the model. Salinity will be affected by fresh water fluxes.
- `STABLERUN` restores sea surface salinity to climatology when salinity is lower than 5 pss

b. Namelist

Namelists related to salinity flux at the sea surface are listed on Tables 14.13 and 14.14.

Table14.13 Namelist `nml_mkflux`. See also Table 14.11.

| variable name | units | description | usage |
|---|---|---|---|
| `rs_local` | | how salinity for iceberg and snow is extracted | 1 : taken from the local grid<br>0 : taken from global sea surface |

Table14.14 Namelist `nml_sss_restore`.

| variable name | units | description | usage |
|---|---|---|---|
| `sss_rst_diff_max` | pss | the maximum of the difference between model and reference sea surface salinity | default = 100 pss |
| `l_nosss_rst_seaice` | logical | no surface salinity restoring below sea ice | default = .`false`. |
| `l_nosss_rst_cstice` | logical | no surface salinity restoring at the coastal grid with sea ice | default = .`false`. |
| `l_sss_rst_cnsv` | logical | set globally integrated surface salinity restoring to zero | default = .`false`. |
| `l_strict_sss_rst_cnsv` | logical | global summation of surface salinity restoring flux is done serially so that the result becomes MPI parallel independent | default = .`false`. |

## 14.9 Bulk transfer coefficient

This section briefly describes how to calculate sea surface fluxes using a bulk formula. For details, readers are referred to Kantha and Clayson (2000), Large and Yeager (2004) and ECMWF (2016b). Bulk transfer coefficient for air-ice interface is given in Section 17.2.1.

### 14.9.1 Formulation of bulk formula

Transfer processes through atmosphere and ocean boundaries are governed by complicated turbulent processes. Traditionally, these turbulent fluxes are parameterized as a bulk transfer law. This method does not explicitly solve the interaction between the atmosphere and the ocean, and attributes all unknown processes to bulk transfer coefficients.

Momentum ($|\overrightarrow{\tau_{AO}}|$), sensible heat ($Q_{SN}$), latent heat ($Q_{LA}$), and water vapor ($E$) fluxes are written in terms of turbulent components as follows:

$$|\overrightarrow{\tau_{AO}}| = -\rho_a \overline{wu} = \rho_a u_*^2, \tag{14.42}$$

$$Q_{SN} = -\rho_a c_{pa} \overline{w\theta} = \rho_a c_{pa} u_* \theta_*, \tag{14.43}$$

$$Q_{LA} = -\rho_a L_E \overline{wq} = \rho_a L_E u_* q_*, \tag{14.44}$$

$$E = -\rho_a \overline{wq} = \rho_a u_* q_* = Q_{LA}/L_E, \tag{14.45}$$

where a bar over two variables denotes a covariance between the turbulent component of vertical velocity ($w$) and that of each physical property, wind speed ($u$), air potential temperature ($\theta$), and specific humidity ($q$). $\rho_a$ is air density, $u_*$ is friction velocity, $\theta_* \equiv Q_{SN}/(\rho_a c_{pa} u_*)$ is the temperature scale in the boundary layer, $q_* \equiv Q_{LA}/(\rho_a L_E u_*) = E/(\rho_a u_*)$ is the scale of specific humidity in the boundary layer, $c_{pa}$ is the specific heat of air, and $L_E$ is the latent heat of water vapor evaporation.

Sea surface fluxes are also represented using bulk formulae as follows:

$$\tau_{AO_x} = \rho_a C_{\mathrm{Dh}} |\vec{U}_a - \vec{U}_s| (U_a - U_s), \tag{14.46}$$

$$\tau_{AO_y} = \rho_a C_{\mathrm{Dh}} |\vec{U}_a - \vec{U}_s| (V_a - V_s), \tag{14.47}$$

$$Q_{SN} = -\rho_a c_{pa} |\vec{U}_a - \vec{U}_s| C_{\mathrm{Hh}} (T_s - \theta_a), \tag{14.48}$$

$$Q_{LA} = -\rho_a L_E |\vec{U}_a - \vec{U}_s| C_{\mathrm{Eh}} (q_s - q_a), \tag{14.49}$$

$$E = \rho_a |\vec{U}_a - \vec{U}_s| C_{\mathrm{Eh}} (q_s - q_a), \tag{14.50}$$

where $\vec{U}_a = (U_a, V_a)$ is the wind vector at a height of $z_{\mathrm{h}}$, $\vec{U}_s = (U_s, V_s)$ is the current vector at the sea surface, $\tau_{AO_x}$ and $\tau_{AO_y}$ are the zonal and meridional component of wind stress $\overrightarrow{\tau_{AO}}$, respectively, and $T_s$ is the absolute sea surface water temperature (K). The subscript "$a$" means the value at a height of $z = z_{\mathrm{h}}$, and the subscript "$s$" means the value at the sea

surface. Specific humidity at sea surface $q_s$ is calculated by Eq. (14.122). The contribution factor ($\alpha$) of the surface current to the calculation of the relative wind vector explained in Section 14.1 is omitted here for brevity.

Parameter $C_{\mathrm{Dh}}$ is called a drag coefficient. $C_{\mathrm{Hh}}$ and $C_{\mathrm{Eh}}$ are transfer coefficients for heat and water vapor and are called the Stanton coefficient and the Dalton coefficient, respectively. These can be estimated by observed atmospheric elements (wind velocity, air temperature, and humidity) at a height in the boundary layer, not by observed turbulent fluxes, using the following Equations (14.51), (14.52), and (14.53) and the similarity law of Monin-Obukhov mentioned below,

$$C_{\mathrm{Dh}} = \frac{u_*^2}{|\vec{U}_a - \vec{U}_s|^2}, \tag{14.51}$$

$$C_{\mathrm{Hh}} = -\frac{Q_{SN}/\rho_a c_{pa}}{|\vec{U}_a - \vec{U}_s|(T_s - \theta_a)} = \frac{u_*\theta_*}{|\vec{U}_a - \vec{U}_s|(T_s - \theta_a)}, \tag{14.52}$$

$$C_{\mathrm{Eh}} = \frac{E/\rho_a}{|\vec{U}_a - \vec{U}_s|(q_s - q_a)} = \frac{u_* q_*}{|\vec{U}_a - \vec{U}_s|(q_s - q_a)}. \tag{14.53}$$

The similarity law of Monin-Obukhov assumes that physical properties in the atmosphere-ocean boundary layer (a layer with a thickness of several tens of meters located below the lower mixed layer of the atmosphere) have similar vertical profiles when they are scaled with the stability parameter and sea surface fluxes. Vertical profiles of wind speed ($U$), air temperature ($\theta$), and humidity ($q$) can be written as follows:

$$\frac{\kappa z}{u_*}\frac{\mathrm{d}U(z)}{\mathrm{d}z} = \phi_M\left(\frac{z}{\mathcal{L}}\right), \tag{14.54}$$

$$\frac{\kappa z}{\theta_*}\frac{\mathrm{d}\theta(z)}{\mathrm{d}z} = \phi_H\left(\frac{z}{\mathcal{L}}\right), \tag{14.55}$$

$$\frac{\kappa z}{q_*}\frac{\mathrm{d}q(z)}{\mathrm{d}z} = \phi_E\left(\frac{z}{\mathcal{L}}\right), \tag{14.56}$$

where $\kappa = 0.4$ is the von Karman constant, and $\mathcal{L}$ is the Monin-Obukhov length scale

$$\mathcal{L} = \frac{u_*^3}{\kappa Q_b} = -\frac{u_*^3\theta_v}{\kappa\, g\, \overline{w\theta_v}}. \tag{14.57}$$

In (14.57), $Q_b = -g\,\overline{w\theta_v}/\theta_v$ is the buoyancy flux, $\theta_v$ is the virtual temperature ($\theta_v = \theta\,(1 + c_{vt}\,q)$; see also (14.134)), and $\overline{w\theta_v}$ is the net heat flux including the water vapor flux:

$$\overline{w\theta_v} = \overline{w\theta}\,(1 + c_{vt}\,q) + c_{vt}\,\theta\,\overline{wq}. \tag{14.58}$$

In (14.54) to (14.56), $\zeta = z/\mathcal{L}$ is the Monin-Obukhov similarity variable, and $\phi_{M,H,E}$ are nondimensional functions for wind velocity, air temperature, and specific humidity. The nondimensional functions are assumed to be mathematically simple functions.

Now we integrate equations (14.54), (14.55), and (14.56) in the vertical direction and gains the following equations:

$$U(z) - U(z_0) = \frac{u_*}{\kappa}\int_{z_0}^{z}\frac{1}{z'}\phi_M\left(\frac{z'}{\mathcal{L}}\right)dz', \tag{14.59}$$

$$\theta(z) - \theta(z_{0\mathrm{T}}) = \frac{\theta_*}{\kappa}\int_{z_{0\mathrm{T}}}^{z}\frac{1}{z'}\phi_H\left(\frac{z'}{\mathcal{L}}\right)dz', \tag{14.60}$$

$$q(z) - q(z_{0\mathrm{E}}) = \frac{\theta_*}{\kappa}\int_{z_{0\mathrm{E}}}^{z}\frac{1}{z'}\phi_E\left(\frac{z'}{\mathcal{L}}\right)dz', \tag{14.61}$$

where $z_0$, $z_{0\mathrm{T}}$, and $z_{0\mathrm{E}}$ are roughness lengths for each physical property. These are the aerodynamic roughness lengths, which are the heights at which each physical characteristic value coincides with the value at the sea level boundary when extrapolated downward based on the Monin-Obukhov similarity law. In short, $U(z_0) = U_s$, $\theta(z_{0\mathrm{T}}) = T_s$, and $q(z_{0\mathrm{E}}) = q_s$. Eqs. (14.59), (14.60), and (14.61) are rewritten as follows:

$$U(z) - U_s = \frac{u_*}{\kappa}\left[\ln\frac{z}{z_0} - \Psi_M(\zeta, \zeta_M)\right], \tag{14.62}$$

$$\theta(z) - T_s = \frac{\theta_*}{\kappa}\left[\ln\frac{z}{z_{0\mathrm{T}}} - \Psi_H(\zeta, \zeta_H)\right], \tag{14.63}$$

$$q(z) - q_s = \frac{q_*}{\kappa}\left[\ln\frac{z}{z_{0\mathrm{E}}} - \Psi_E(\zeta, \zeta_E)\right], \tag{14.64}$$

where

$$\Psi_{M,H,E}(\zeta,\zeta_{M,H,E}) = \int_{\zeta_{M,H,E}}^{\zeta} \left[1-\phi_{M,H,E}(\zeta')\right]\frac{d\zeta'}{\zeta'}. \tag{14.65}$$

The lower ends of the integral in (14.65), $\zeta_M$, $\zeta_H$ and $\zeta_E$ are calculated as $z_0/\mathcal{L}$, $z_{0T}/\mathcal{L}$ and $z_{0E}/\mathcal{L}$, respectively. When the stability of the boundary layer ($\zeta$) is already known, bulk transfer coefficients can be estimated from the equations (14.51, 14.52, 14.53) using these roughness lengths and the relationships $U_a = U(z_h), \theta_a = \theta(z_h), q_a = q(z_h)$,

$$C_{\mathrm{Dh}} = \frac{\kappa^2}{\left[\ln\frac{z_\mathrm{h}}{z_0} - \Psi_M(\zeta_h,\zeta_M)\right]^2}, \tag{14.66}$$

$$C_{\mathrm{Hh,Eh}} = \frac{\kappa^2}{\left[\ln\frac{z_\mathrm{h}}{z_0} - \Psi_M(\zeta_h,\zeta_M)\right]\left[\ln\frac{z_\mathrm{h}}{z_{0\mathrm{T,0E}}} - \Psi_{H,E}(\zeta_h,\zeta_{H,E})\right]}. \tag{14.67}$$

### 14.9.2 Large and Yeager (2004; 2009): BULKNCAR

In neutral stability, $\phi_{M,H,E} = 1$ gives a good approximation for Eqs. (14.54), (14.55) and (14.56). Then, the equation (14.65) gives $\Psi_{M,H,E} = 0$. The bulk transfer coefficient is a function of the roughness length ($z_0$,$z_{0T}$, and $z_{0E}$ for each) only and is expressed as follows:

$$C_{\mathrm{DNh}} = \frac{\kappa^2}{\left[\ln\frac{z_\mathrm{h}}{z_0}\right]^2}, \tag{14.68}$$

$$C_{\mathrm{HNh,ENh}} = \frac{\kappa^2}{\left[\ln\frac{z_\mathrm{h}}{z_0}\right]\left[\ln\frac{z_\mathrm{h}}{z_{0\mathrm{T,0E}}}\right]} \tag{14.69}$$

$$= \frac{C_{\mathrm{DNh}}}{\left[1-\frac{1}{\kappa}C_{\mathrm{DNh}}^{1/2}\ln\frac{z_{0\mathrm{T,0E}}}{z_0}\right]} \tag{14.70}$$

$$= \frac{\kappa C_{\mathrm{DNh}}^{1/2}}{\left[\ln\frac{z_\mathrm{h}}{z_{0\mathrm{T,0E}}}\right]}. \tag{14.71}$$

Normally, these neutral bulk transfer coefficients are estimated at a height of 10 m. Non-neutral bulk transfer coefficients at an arbitrary height ($z_\mathrm{h}$) are connected with the neutral bulk transfer coefficients at a height of 10 m as follows:

$$C_{\mathrm{Dh}} = \frac{C_{\mathrm{DN10}}}{\left[1+\frac{1}{\kappa}C_{\mathrm{DN10}}C_{\mathrm{DN10}}^{-1/2}\left(\ln\frac{z_\mathrm{h}}{z_{10}} - \Psi_M(\zeta_h)\right)\right]^2}, \tag{14.72}$$

$$C_{\mathrm{Hh,Eh}} = \frac{C_{\mathrm{HN10,EN10}}\left(\frac{C_{\mathrm{Dh}}}{C_{\mathrm{DN10}}}\right)^{1/2}}{\left[1+\frac{1}{\kappa}C_{\mathrm{HN10,EN10}}C_{\mathrm{DN10}}^{-1/2}\left(\ln\frac{z_\mathrm{h}}{z_{10}} - \Psi_{H,E}(\zeta_h)\right)\right]}, \tag{14.73}$$

where $z_{10}$ means $z = 10\,\mathrm{m}$. If we approximate $\zeta_{M,H,E}$ by zero in Eq. (14.65), the equations above are independent from the roughness length.

The neutral bulk transfer coefficients at a height of 10 m ($C_{\mathrm{DN10}}$, $C_{\mathrm{HN10}}$, and $C_{\mathrm{EN10}}$) are often estimated, according to the stability, as a function of velocity at 10 m. In the bulk formula based on Large and Yeager (2004; 2009), the bulk transfer coefficient at 10 m in the neutral stability is given as follows:

$$10^3 C_{\mathrm{DN10}} = \begin{cases} \frac{2.70}{U_{10\mathrm{N}}} + 0.142 + \frac{U_{10\mathrm{N}}}{13.09} - 3.14807\times10^{-10}U_{10\mathrm{N}}^6, & U_{10\mathrm{N}} < 33\,\mathrm{m\,s^{-1}} \\ 2.34 & U_{10\mathrm{N}} \geq 33\,\mathrm{m\,s^{-1}} \end{cases} \tag{14.74}$$

$$10^3 C_{\mathrm{EN10}} = 34.6\sqrt{C_{\mathrm{DN10}}}, \tag{14.75}$$

$$10^3 C_{\mathrm{HN10}} = \begin{cases} 18.0\sqrt{C_{\mathrm{DN10}}}, & \text{stable } \zeta > 0, \\ 32.7\sqrt{C_{\mathrm{DN10}}}, & \text{unstable } \zeta \le 0, \end{cases} \tag{14.76}$$

Each turbulent flux is estimated at a height where wind speed is observed by transforming air temperature and humidity from the height where they are observed ($z_\theta$ and $z_q$, respectively) to the height where wind speed is observed. The observed heights are specified in namelist `nml_srfflx_dbase` (see Table 14.20).

Each physical property is estimated at a height where wind speed is observed in the following operations. First, calculate the virtual temperature $\theta_v$ according to (14.134) with air temperature at $z_\theta$ and specific humidity at $z_q$ as follows:

$$\theta_v = \theta(z_\theta)(1 + c_{vt}\, q(z_q)) \tag{14.77}$$

Next, calculate the bulk transfer coefficient at 10 m in the neutral stability assuming that the first guess for the 10 m wind speed in the neutral stability is $U_{10\mathrm{N}} = |\Delta\vec{U}(z_u)| = |\vec{U}_a(z_u) - \vec{U}_s|$ (Equations (14.74) to (14.76)). The first guesses of the scales for the friction velocity, air temperature, and specific humidity are estimated assuming that these bulk coefficients are at the observed height and stability,

$$u_* = \sqrt{\frac{|\overrightarrow{\tau_{AO}}|}{\rho_a}} = \sqrt{C_{\mathrm{DN10}}}\,|\Delta\vec{U}(z_u)|, \tag{14.78}$$

$$\theta_* = \frac{Q_{SN}}{\rho_a c_p u_*} = \frac{C_{\mathrm{HN10}}}{\sqrt{C_{\mathrm{DN10}}}}\,(\theta(z_\theta) - T_s), \tag{14.79}$$

$$q_* = \frac{E}{\rho_a u_*} = \frac{C_{\mathrm{EN10}}}{\sqrt{C_{\mathrm{DN10}}}}\,(q(z_q) - q_s), \tag{14.80}$$

where $q_s$ is the saturated specific humidity at sea surface temperature $T_s$.

Next, perform the iteration using the three Monin-Obukhov similarity variables, $\zeta_u = z_u/\mathcal{L}$, $\zeta_\theta = z_\theta/\mathcal{L}$, and $\zeta_q = z_q/\mathcal{L}$, and an integral of the nondimensional profile function for the vertical gradient of each physical property, $\Psi_M(\zeta)$ for momentum and $\Psi_H(\zeta)$ for scalars.

The Monin-Obukhov similarity variables are calculated as follows:

$$\zeta = \frac{\kappa g z}{u_*^2}\left[\frac{\theta_*}{\theta_v} + \frac{q_*}{(q(z_q) + c_{vt}^{-1})}\right]. \tag{14.81}$$

The integral of the non-dimensional profile function is expressed as

$$\Psi_M(\zeta) = \Psi_H(\zeta) = -5\zeta, \tag{14.82}$$

if it is stable ($\zeta \ge 0$), and

$$\Psi_M(\zeta) = 2\ln\left(\frac{1+X}{2}\right) + \ln\left(\frac{1+X^2}{2}\right) - 2\tan^{-1}(X) + \frac{\pi}{2}, \tag{14.83}$$

$$\Psi_H(\zeta) = 2\ln\left(\frac{1+X^2}{2}\right), \tag{14.84}$$

if it is unstable ($\zeta < 0$). In the above,

$$X = (1 - 16\zeta)^{1/4}. \tag{14.85}$$

Using these values, convert the wind speed to that at 10 m in the neutral stability, and convert the temperature and specific humidity to those at a height where the wind speed is observed,

$$U_{10\mathrm{N}} = |\Delta\vec{U}(z_u)|\left(1 + \frac{\sqrt{C_{\mathrm{DN10}}}}{\kappa}\left[\ln\frac{z_u}{z_{10}} - \Psi_M(\zeta_u)\right]\right)^{-1}, \tag{14.86}$$

$$\theta(z_u) = \theta(z_\theta) - \frac{\theta_*}{\kappa}\left[\ln\frac{z_\theta}{z_u} + \Psi_H(\zeta_u) - \Psi_H(\zeta_\theta)\right], \tag{14.87}$$

$$q(z_u) = q(z_q) - \frac{q_*}{\kappa}\left[\ln\frac{z_q}{z_u} + \Psi_H(\zeta_u) - \Psi_H(\zeta_q)\right], \tag{14.88}$$

where $z_{10}$ means $z = 10\,\mathrm{m}$. Estimate the bulk coefficient at 10 m in the neutral stability using $U_{10\mathrm{N}}$, and then obtain the bulk coefficient at a height ($z_u$) where wind speed is observed,

$$C_{\mathrm{Du}} = \frac{C_{\mathrm{DN10}}}{\left[1 + \frac{1}{\kappa} C_{\mathrm{DN10}} C_{\mathrm{DN10}}^{-1/2} \left(\ln \frac{z_u}{z_{10}} - \Psi_M(\zeta_u)\right)\right]^2}, \tag{14.89}$$

$$C_{\mathrm{Hu}} = \frac{C_{\mathrm{HN10}} \left(\frac{C_{\mathrm{Du}}}{C_{\mathrm{DN10}}}\right)^{1/2}}{\left[1 + \frac{1}{\kappa} C_{\mathrm{HN10}} C_{\mathrm{DN10}}^{-1/2} \left(\ln \frac{z_u}{z_{10}} - \Psi_H(\zeta_u)\right)\right]}, \tag{14.90}$$

$$C_{\mathrm{Eu}} = \frac{C_{\mathrm{EN10}} \left(\frac{C_{\mathrm{Du}}}{C_{\mathrm{DN10}}}\right)^{1/2}}{\left[1 + \frac{1}{\kappa} C_{\mathrm{EN10}} C_{\mathrm{DN10}}^{-1/2} \left(\ln \frac{z_u}{z_{10}} - \Psi_H(\zeta_u)\right)\right]}. \tag{14.91}$$

Repeat the procedures to calculate the bulk coefficients using these bulk coefficients with temperature and specific humidity at $z = z_u$, and recalculate virtual temperature (14.134) and the scales for friction velocity, temperature, and specific humidity (Equations of (14.78), (14.79), and (14.80)). Note that Large and Yeager (2004) recommend to use a bulk water temperature a meter of more beneath the sea surface as sea surface temperature $T_s$ in Eq. (14.48) because their formulation is based on fitting to observation data using a bulk water temperature not a skin temperature.

### 14.9.3 ECMWF (2016): BULKECMWF

Bulk formulae of Integrated Forecasting System (IFS) developed in European Centre for Medium-Range Weather Forecasts (ECMWF) (ECMWF, 2016b) are also available in MRI.COM. Bulk transfer coefficients are calculated by Eqs. (14.66) and (14.67). Turbulent surface fluxes are calculated as follows:

$$\tau_{AO_x} = \rho_a C_{\mathrm{Dh}} |U_{\mathrm{rel}}| (U_a - U_s), \tag{14.92}$$

$$\tau_{AO_y} = \rho_a C_{\mathrm{Dh}} |U_{\mathrm{rel}}| (V_a - V_s), \tag{14.93}$$

$$Q_{SN} = -\rho_a c_{pa} |U_{\mathrm{rel}}| C_{\mathrm{Hh}} (\theta_{vs} - \theta_v), \tag{14.94}$$

$$Q_{LA} = -\rho_a L_E |U_{\mathrm{rel}}| C_{\mathrm{Eh}} (q_s - q_a), \tag{14.95}$$

$$E = \rho_a |U_{\mathrm{rel}}| C_{\mathrm{Eh}} (q_s - q_a), \tag{14.96}$$

where $|U_{\mathrm{rel}}|$ denotes wind speed in the atmosphere bottom layer. This wind speed is calculated as follows:

$$|U_{\mathrm{rel}}| = \left(|\vec{U}_a - \vec{U}_s|^2 + w_\dagger^2\right)^{\frac{1}{2}}, \tag{14.97}$$

where $w_\dagger$ is a vertical velocity scale which parameterizes vertical motion associate with the free convection due to heating. The sensible flux $Q_{SN}$ (14.94) is calculated from the virtual temperature $\theta_v$ and $\theta_{vs}$. Those are the virtual temperature in the atmosphere bottom layer and that at the sea surface calculated with skin temperature $T_{\mathrm{skin}}$, respectively. Note that the skin temperature usually differs from sea water temperature in the top layer of the ocean model. Details about calculation of $w_\dagger$, the virtual temperature and $T_{\mathrm{skin}}$ are described afterward.

The calculation procedures are summarized as follows.

1. Calculate the skin temperature (14.9.3a)
2. Read the free convection velocity scale ($w_\dagger$) at the previous time step
3. Calculate the wind speed in the atmosphere bottom layer ($|U_{\mathrm{rel}}|$)
4. Calculate bulk Richardson number (14.9.3b)
5. Read friction velocity ($u_*$) at the previous time step
6. Initialize Monin-Obukhov length
7. Calculate the bulk transfer coefficients by iteration method (repeat the following procedures `itr_z0_num` times)
   (a) Calculate roughness length $z_{0,0T,0E}$ from the friction velocity (14.9.3c)
   (b) Calculate the Monin-Obukhov length (14.9.3d)
   (c) Calculate the bulk transfer coefficients (14.66 and 14.67)
   (d) Calculate the friction velocity $u_*$ from the bulk transfer coefficient of momentum $C_{\mathrm{Dh}}$ (14.9.3e)

8. Calculate the surface turbulent fluxes using bulk transfer coefficients
9. Calculate the free convection velocity scale $w_\dagger$ from the sensible and latent heat fluxes for the next time step (14.9.3f)

The free convection velocity scale $w_\dagger$ is assumed to be zero when its value at the previous step is unknown in the procedure (2). When the friction velocity $u_*$ at the previous step is not available in the procedure (5), it is calculated by Eq. (14.117) described afterward with $C_{\mathrm{Dh}} = 0.001$. The Monin-Obukhov length $\mathcal{L}$ also requires initialization in the procedure (6). Its initial value is calculated as follows:

$$\frac{1}{\mathcal{L}} = \begin{cases} \exp\left(Ri_{bulk}/3 + 1\right) - 1.5 & (Ri_{bulk} < Ri_{lim}), \\ \zeta_{lim}/z_h & (otherwise). \end{cases} \tag{14.98}$$

This bulk formulae assume that the marine meteorological properties are observed at the same height. The observed height is specified by `alt_wind_meter` in namelist `nml_srfflx_dbase`. The other parameters `alt_temp_meter` and `alt_sphm_meter` are neglected and not used in the current formulae. Users may specify coefficients of the hybrid vertical coordinate in the bottom layer of the IFS atmosphere model. Then, the observed height is diagnosed from sea level pressure and the virtual temperature in the atmosphere bottom layer according to the equation below (ECMWF, 2016a):

$$z_h = \frac{R_{dry}\theta_v}{g}\left[1 - \frac{p_t}{p_s - p_t}\ln\left(\frac{p_s}{p_t}\right)\right], \tag{14.99}$$

where $R_{dry}$ is the gas constants for dry air and $p_s$ and $p_t$ are the sea level pressure and pressure at the top interface of the atmosphere bottom layer, respectively. The top-interface pressure $p_t$ is calculated as follows:

$$p_t = A + Bp_s. \tag{14.100}$$

The coefficients $A$ and $B$ are specified in namelist `nml_bulkecmwf`.

### a. Calculation of skin temperature

The current bulk formulae use the skin temperature $T_{\mathrm{skin}}$ and it usually differs from the top-layer temperature of the ocean model. MRI.COM adopts a simple skin layer scheme implemented in the Japan Meteorological Agency's global atmosphere model. The skin temperature $T_{\mathrm{skin}}$ is calculated as follows:

$$T_{\mathrm{skin}} = T_o + \Delta T, \tag{14.101}$$

$$\Delta T = \max\left[0, \frac{Q_{SH}(z=\eta) + Q_{LO}^{\mathrm{net}}}{500}\cdot f_{wind}\right], \tag{14.102}$$

$$f_{wind} = \max\left[0.2, \frac{10 - |\vec{U}_a - \vec{U}_s|}{10}\right], \tag{14.103}$$

where $T_o$ denotes the ocean top-layer potential temperature, $Q_{SH}(z=\eta)$ (14.3) and $Q_{LO}{}^{\mathrm{net}}$ (14.27) are net downward shortwave and net downward longwave at the sea surface in units of $\mathrm{W/m^2}$, respectively, and $|\vec{U}_a - \vec{U}_s|$ is relative wind speed in units of $\mathrm{m/s}$.

### b. Calculation of bulk Richardson number

The following equation gives the bulk Richardson number:

$$Ri_{bulk} = \left(\frac{g}{\overline{\theta_v}}\right)\frac{z_h(\theta_v - \theta_{vs})}{|U_{\mathrm{rel}}|^2}, \tag{14.104}$$

where $\theta_v$ and $\theta_{vs}$ denote the virtual temperature at the height of $z = z_h$ and the sea level (14.134). They are calculated as follows:

$$\theta_v = \theta_a(1 + c_{vt}q_a), \tag{14.105}$$

$$\theta_{vs} = T_{\mathrm{skin}}(1 + c_{vt}q_s), \tag{14.106}$$

where $\overline{\theta_v}$ is mean virtual temperature within the atmosphere bottom layer, which is given by $\overline{\theta_v} = 0.5(\theta_v + \theta_{vs})$.

c. Calculation of roughness length

The roughness lengths over the sea are calculated by the following equation with the friction velocity $u_*$:

$$z_0 = \alpha_M \frac{\nu}{u_*} + \alpha_{Ch} \frac{u_*^2}{g}, \tag{14.107}$$

$$z_{0T,0E} = \alpha_{H,E} \frac{\nu}{u_*}, \tag{14.108}$$

where $\alpha_M = 0.11, \alpha_H = 0.40, \alpha_E = 0.62$, $\nu$ is kinematic viscosity coefficient ($\nu = 1.5 \times 10^{-5} m^2 s^{-1}$), and $\alpha_{Ch}$ is the Charnock coefficient ($\alpha_{Ch} = 0.018$).

d. Calculation of the Monin-Obukhov length

The Monin-Obukhov length is calculated from the bulk Richardson number $Ri_{bulk}$. A stability parameter $\zeta = z/\mathcal{L}$ is associated with the bulk Richardson number as follows:

$$Ri_{bulk} = \zeta \cdot \frac{\left[\ln\left(\frac{z_h}{z_{0H}}\right) - \Psi_H\left(\zeta_h, \zeta_H\right)\right]}{\left[\ln\left(\frac{z_h}{z_{0M}}\right) - \Psi_M\left(\zeta_h, \zeta_M\right)\right]^2}. \tag{14.109}$$

When the bulk Richardson number calculated by Eq. (14.104) goes below the upper limit $Ri_{lim} = 6$, the Monin-Obukhov length is calculated by solving Eq. (14.109) with iteration method. The inverse of the Monin-Obukhov length is iteratively recalculated by the following equation:

$$\frac{1}{\mathcal{L}} = \frac{Ri_{bulk}\left[\ln\left(\frac{z_h}{z_{0M}}\right) - \Psi_M\left(\zeta_h, \zeta_M\right)\right]^2}{z_h\left[\ln\left(\frac{z_h}{z_{0H}}\right) - \Psi_H\left(\zeta_h, \zeta_H\right)\right]}. \tag{14.110}$$

The iteration stops if the bulk Richardson number calculated by Eq. (14.109) matches the value calculated by Eq. (14.104) within a predetermined error range or the iteration count exceeds the maximum number.

When the bulk Richardson number calculated by Eq. (14.104) is larger than $Ri_{lim}$ or the Monin-Obukhov length calculated above satisfies $\zeta_h = z_h/\mathcal{L} > \zeta_{lim} = 0.5$, the Monin-Obukhov length is given by the following equation:

$$\frac{1}{\mathcal{L}} = \frac{\zeta_{lim}}{z_h}. \tag{14.111}$$

Stability functions $\Psi_{M,H,E}$ are calculated as follows:

$$\Psi_{M,H,E}(\zeta_h, \zeta_{M,H,E}) = \psi_{M,H,E}(\zeta_h) - \psi_{M,H,E}(\zeta_{M,H,E}). \tag{14.112}$$

Under unstable conditions ($\zeta < 0$),

$$\psi_M(\zeta) = \frac{\pi}{2} - 2\,\mathrm{atan}(X) + \ln\frac{(1+X)^2(1+X^2)}{8}, \tag{14.113}$$

$$\psi_{H,E}(\zeta) = 2\ln\left(\frac{1+X^2}{2}\right), \tag{14.114}$$

where $X = (1 - 16\zeta)^{1/4}$. Under stable conditions ($\zeta > 0$),

$$\psi_M(\zeta) = -b\left(\zeta - \frac{c}{d}\right)\exp(-d\zeta) - a\zeta - \frac{bc}{d}, \tag{14.115}$$

$$\psi_{H,E}(\zeta) = -b\left(\zeta - \frac{c}{d}\right)\exp(-d\zeta) - \left(1 + \frac{2}{3}a\zeta\right)^{1.5} - \frac{bc}{d} + 1, \tag{14.116}$$

where $a = 1, b = 2/3, c = 5$, and $d = 0.35$.

e. Calculation of friction velocity

The following equation gives the friction velocity with the bulk transfer coefficient of momentum $C_{\mathrm{Dh}}$:

$$u_* = C_{\mathrm{Dh}}^{\frac{1}{2}} |U_{\mathrm{rel}}|. \tag{14.117}$$

f. Calculation of free-convection velocity scale $w_\dagger$

As noted above, the current bulk formulae take the free-convection velocity $w_\dagger$ into account for the wind speed of the atmosphere bottom layer. This velocity scale is calculated as follows:

$$w_\dagger = \left( z_i \frac{g}{\theta_a} Q_{ov} \right)^{\frac{1}{3}}, \tag{14.118}$$

$$Q_{ov} = \frac{Q_{SN}}{\rho_a c_{pa}} + \frac{c_{vt} \theta_a E}{\rho_a}, \tag{14.119}$$

where $c_{vt} = m_\mathrm{a}/m_\mathrm{w} - 1 = R_{vap}/R_{dry} - 1$ (see (14.135)), $R_{vap}(m_\mathrm{w})$ and $R_{dry}(m_\mathrm{a})$ are the gas constants (mean molecular weights) for water vapor and dry air, respectively, $z_i = 1000$ m, $Q_{SN}$ denotes the sensible heat flux calculated by Eq. (14.94), and $E$ is the water vapor flux calculated by Eq. (14.96). We use the surface fluxes $Q_{SN}$ and $E$ calculated at the previous step there.

### 14.9.4 Usage

a. Model option

- `BULKNCAR` for Large and Yeager (2004; 2009)
- `BULKECMWF` and `SKINGSAM` for ECMWF (2016b)

b. Namelist

Tables 14.15 and 14.16 show namelists available when `BULKECMWF` is specified.

Table14.15 Namelist `nml_bulkecmwf`)

| variable name | units | description | usage |
|---|---|---|---|
| `itr_z0_num` | 1 | The number of iteration of roughness length calculation | default = 5 |
| `l_bulkecmwf_calc_altitude` | logical | Calculate the observed height of marine meteorological properties | default = `.true.` |
| `a_sfc_layer` | Pa | Coefficient $A$ in Eq. (14.100) | default = 0.00316 |
| `b_sfc_layer` | 1 | Coefficient $B$ in Eq. (14.100) | default = 0.99763 |
| `l_GSAM_compatible` | logical | Use a parameter set used in the Japan Meteorological Agency's global atmosphere model GSM1705 | default = `.false.` |

Table14.16 Namelist `nml_bulkecmwf_ocn_run`)

| variable name | units | description | usage |
|---|---|---|---|
| `l_rst_bulkecmwf_ocn_in` | logical | read initial restart for the friction velocity and the free convection velocity scale or not | default = `l_rst_in` |

## 14.10 Specification of input data

The attributes of external forcing data should be specified by namelist `nml_force_data`. Table 14.17 explains variables that are contained in this namelist block.

Table14.17 Namelist nml_force_data related to surface forcing data.

| variable name | units | description | usage |
|---|---|---|---|
| name | | name of data object | |
| txyu | | grid point on which data should be placed | |
| l2d | logical | data is 2D or not | .true. for surface data, default = .false.) |
| file_data | | file that contains reference vales for surface restoring forcing | |
| file_data_grid | | data file name of grid | needed if linterp = .true. |
| imfrc | | grid number of data in x direction | |
| jmfrc | | grid number of data in y direction | |
| num_elm | | the number of elements contained in file | |
| interval | sec | regular time interval of data | −1 : monthly<br>−999 : steady forcing |
| num_data_max | | the number of record contained in the file | |
| ifstart | ifstart(6) | [ymdhms] of the first record of the input file | |
| lrepeat | logical | repeat use of climatological data or not | default = .false. |
| linterp | logical | interpolate horizontally or not | default = .false. |
| ilinear | | interpolation method | 1 : linear, 2 : spline |
| luniform | logical | data is horizontally uniform or not | default = .false. |
| loffset | logical | data is offset or not | default = .false. |
| offset | | offsetting factor | |
| lfactor | logical | data is multiplied or not | default = .false. |
| factor | | multiplicative factor | |
| ldouble | logical | input data is double precision or not | default = .false. |
| iverbose | | standard output of progress | 1 : extensive, 0 : minimum |
| ldefined | logical | data object with this name is defined or not | default = .true. |

Format of data files that should be prepared is shown in the following. Note that one data file should contain only one element.

Format of surface forcing data (trcref(_surf)_conf%file_data)

```
integer(4), parameter :: num_data_max = 365*4, nu = 99
          ! "num_data_max" is  the number of data
integer(4) :: imfrc, jmfrc    ! data size
character(128) :: file_data, file_data_grid
real(4) :: precip(imfrc,jmfrc,num_data_max)
real(8) :: alonf(imfrc), alatf(jmfrc)
logical :: linterp

! main data

open (unit=nu,file=file_data,access=direct,recl=4*imfrc*jmfrc)
do n = 1, num_data_max
  write(unit=nu,rec=n) precip(:,:,n)
end do
close(nu)

! longitude/latitude of the main data

if (linterp) then  ! If input data is horizontally interpolated in the model.
  open (unit=nu,file=file_grid)
  write(nu) alonf, alatf
  close(nu)
end if
```

## 14.11 Surface data objects

External data either read from file or received from AGCM are stored in the data set object type `type_surf_dbase` (Table 14.18). This object contains a sub object `meteor_alt` of type `type_surf_meteor_alt` (Table 14.19) that stores the measurement height of marine meteorological variables. The name (`ReadData` for Reanalysis or `FromCGCM` for AGCM) of the object and the measurement height of marine meteorological variables must be specified by namelist `nml_srfflx_dbase` (Table 14.20).

Air-sea fluxes computed on the basis of external data are stored in the data set object type `type_surf_product_ao` (Table 14.21). This object contains sub objects `givn_ao` and `calc_ao` of the object type `type_surf_bulk_ao` (Table 14.22). The object `calc_ao` stores elements related to the computation of fluxes based on the bulk formula and the object `givn_ao` stores the corresponding elements received by other components, that is, atmospheric model. Similarly, air-ice fluxes are stored in `type_surf_product_ai` (Table 14.23), which contains sub objects `givn_ai` and `calc_ai` of the object type `type_surf_bulk_ai` (Table 14.24).

Table14.18 Contents of the object `type_surf_dbase` related to external surface forcing data.

| variable name | units | description |
|---|---|---|
| `name` | | name of data object |
| `meteor_alt` | `type_surf_meteor_alt` | Observation altitude of this data set |
| `x_wind` | $\mathrm{cm\,sec^{-1}}$ or $\mathrm{dyn\,cm^{-2}}$ | X-ward wind or wind stress |
| `y_wind` | $\mathrm{cm\,sec^{-1}}$ or $\mathrm{dyn\,cm^{-2}}$ | Y-ward wind or wind stress |
| `temp_air` | °C | surface air temperature |
| `tdew_air` | °C | dew point temperature |
| `sphm_air` | 1 | specific humidity |
| `s_wind` | $\mathrm{cm\,sec^{-1}}$ | scalar surface wind |
| `slpress` | hPa | sea level pressure |
| `sw_flx` | $\mathrm{erg\,s^{-1}\,cm^{-2}}$ | upward or downward shortwave, summed |
| `sw_flx_visb` | $\mathrm{erg\,s^{-1}\,cm^{-2}}$ | upward or downward shortwave, visible, beam |
| `sw_flx_visd` | $\mathrm{erg\,s^{-1}\,cm^{-2}}$ | upward or downward shortwave, visible, diffuse |
| `sw_flx_nirb` | $\mathrm{erg\,s^{-1}\,cm^{-2}}$ | upward or downward shortwave, near Infra-red, beam |
| `sw_flx_nird` | $\mathrm{erg\,s^{-1}\,cm^{-2}}$ | upward or downward shortwave, near Infra-red, diffuse |
| `lw_flx` | $\mathrm{erg\,s^{-1}\,cm^{-2}}$ | upward or downward longwave |
| `sst` | °C | sea surface temperature |
| `precip` | $\mathrm{cm\,s^{-1}}$ | precipitation water flux |
| `river_w` | $\mathrm{cm\,s^{-1}}$ | river discharge water flux |
| `river_h` | $\mathrm{erg\,s^{-1}\,cm^{-2}}$ | river discharge heat flux |
| `snowfall` | $\mathrm{cm\,s^{-1}}$ | snow fall water flux |
| `iceberg_w` | $\mathrm{cm\,s^{-1}}$ | iceberg discharge water flux |
| `iceberg_h` | $\mathrm{erg\,s^{-1}\,cm^{-2}}$ | iceberg discharge heat flux |
| `frac_ice` | 1 | sea ice fraction |

Table14.19 Contents of the object `type_surf_meteor_alt` that stores measurement height of meteorological elements of external data.

| variable name | units | description |
|---|---|---|
| `alt_wind` | m | altitude of wind |
| `alt_temp` | m | altitude of temperature |
| `alt_sphm` | m | altitude of specific humidity |

Table14.20 Namelist `nml_srfflx_dbase`.

| variable name | units | description | usage |
|---|---|---|---|
| `name` | | name of the external dataset | `ReadData` (Reanalysis) or `FromCGCM` (AGCM) (required) |

Continued on next page

Table 14.20 – continued from previous page

| variable name | units | description | usage |
|---|---|---|---|
| l_marine_meteor | logical | read marine meteorological data or not | required |
| alt_wind_meter | m | observed height of wind | required if l_marine_meteor = .true. |
| alt_temp_meter | m | observed height of temperature | required if l_marine_meteor = .true. |
| alt_sphm_meter | m | observed height of specific humidity | required if l_marine_meteor = .true. |

Table14.21 Contents of the object type_surf_product_ao that stores air-sea fluxes based on type_surf_dbase.

| variable name | units | description |
|---|---|---|
| name | | name of data object |
| l_calc_wind_stress | logical | calculate wind stress for this data set |
| l_calc_bulk_fluxes | logical | calculate fluxes based on a bulk formula for this data set |
| sw_nt_ao | $\mathrm{erg\,s^{-1}\,cm^{-2}}$ | net shortwave, summed |
| sw_nt_visb_ao | $\mathrm{erg\,s^{-1}\,cm^{-2}}$ | net shortwave, visible, beam |
| sw_nt_visd_ao | $\mathrm{erg\,s^{-1}\,cm^{-2}}$ | net shortwave, visible, diffuse |
| sw_nt_nirb_ao | $\mathrm{erg\,s^{-1}\,cm^{-2}}$ | net shortwave, near Infra-red, beam |
| sw_nt_nird_ao | $\mathrm{erg\,s^{-1}\,cm^{-2}}$ | net shortwave, near Infra-red, diffuse |
| lw_nt_ao | $\mathrm{erg\,s^{-1}\,cm^{-2}}$ | net longwave, air-ocean |
| tsfc_ocn | °C | sea surface (skin) temperature |
| wind_speed | $\mathrm{cm\,sec^{-1}}$ | scalar wind speed |
| givn_ao | type_surf_bulk_ao | given from other model or forcing data file |
| calc_ao | type_surf_bulk_ao | calculated using bulk formulae |

Table14.22 Contents of the object `type_surf_bulk_ao` that stores elements related to computation of air-sea fluxes based on bulk formula.

| variable name | units | description |
|---|---|---|
| `name` | | name of data object |
| `x_rel_wind` | $m\,sec^{-1}$ | surface wind relative to surface current |
| `y_rel_wind` | $m\,sec^{-1}$ | surface wind relative to surface current |
| `x_stress` | $dyn\,cm^{-2}$ | X-ward surface stress |
| `y_stress` | $dyn\,cm^{-2}$ | Y-ward surface stress |
| `frcvl` | $m\,sec^{-1}$ | friction velocity |
| `rel_wind` | $m\,sec^{-1}$ | surface wind relative to surface current |
| `latent` | $erg\,s^{-1}\,cm^{-2}$ | latent heat flux, air-ocean |
| `sensible` | $erg\,s^{-1}\,cm^{-2}$ | sensible heat flux, air-ocean |
| `evapo` | $cm\,sec^{-1}$ | evaporative water flux, air-ocean |

Table14.23 Contents of the object `type_surf_product_ai` that stores air-ice fluxes based on `type_surf_dbase`.

| variable name | units | description |
|---|---|---|
| `name` | | name of data object |
| `l_calc_wind_stress` | logical | calculate wind stress for this data set |
| `l_calc_bulk_fluxes` | logical | calculate fluxes based on a bulk formula for this data set |
| `sw_nt_ai` | $erg\,s^{-1}\,cm^{-2}$ | net shortwave, summed, absorbed at the ice surface |
| `sw_nt_in` | $erg\,s^{-1}\,cm^{-2}$ | net shortwave, summed, penetrate into the ice interior |
| `sw_nt_visb_ai` | $erg\,s^{-1}\,cm^{-2}$ | net shortwave, visible, beam |
| `sw_nt_visd_ai` | $erg\,s^{-1}\,cm^{-2}$ | net shortwave, visible, diffuse |
| `sw_nt_nirb_ai` | $erg\,s^{-1}\,cm^{-2}$ | net shortwave, near Infra-red, beam |
| `sw_nt_nird_ai` | $erg\,s^{-1}\,cm^{-2}$ | net shortwave, near Infra-red, diffuse |
| `lw_nt_ai` | $erg\,s^{-1}\,cm^{-2}$ | net longwave, air-ice |
| `tsfc_ice` | °C | ice surface temperature |
| `wind_speed` | $m\,sec^{-1}$ | scalar wind speed |
| `givn_ai` | `type_surf_bulk_ai` | given from other model or forcing data file |
| `calc_ai` | `type_surf_bulk_ai` | calculated using bulk formulae |

Table14.24 Contents of the object `type_surf_bulk_ai` that stores elements related to computation of air-ice fluxes based on bulk formula.

| variable name | units | description |
|---|---|---|
| `name` | | name of data object |
| `x_rel_wind` | $m\,sec^{-1}$ | surface wind relative to ice drift |
| `y_rel_wind` | $m\,sec^{-1}$ | surface wind relative to ice drift |
| `x_stress` | $dyn\,cm^{-2}$ | X-ward surface stress |
| `y_stress` | $dyn\,cm^{-2}$ | Y-ward surface stress |
| `frcvl` | $m\,sec^{-1}$ | friction velocity |
| `rel_wind` | $m\,sec^{-1}$ | surface wind relative to ice drift |
| `latent` | $W\,m^{-2}$ | latent heat flux, air-ice |
| `sensible` | $W\,m^{-2}$ | sensible heat flux, air-ice |
| `sublim` | $m\,sec^{-1}$ of sea water | sublimation water flux, air-ice |
| `ctntmp` | $m\,sec^{-1}$ | bulk transfer coefficient × scalar wind |
| `csntmp` | $m\,sec^{-1}$ | bulk transfer coefficient × scalar wind |

## 14.12 Technical details

### 14.12.1 Recalculating and replacing fluxes in the coupled mode

The ocean model usually receives the surface fluxes calculated in the atmosphere model in the coupled mode (Chapter 21). In coupled mode (`SCUPCGCM` option) or in child mode of nesting (`SUB` option) in which fluxes are taken from the parent model (`NGETFLUX` option which is often used when the parent model is coupled with the atmosphere), this

received fluxes may be replaced by the ones calculated on its own by using the surface atmospheric states taken from the parent component, its surface oceanic states, and its bulk formula. User may also specify the grid points where fluxes are replaced. This option is mainly intended to be applied to coastal region of a child model of nesting in which the fluxes received from the parent component may not fully reflect the fine scale surface state due to complex topography. Without an appropriate feedback mechanism at the sea surface, a child model may sometimes get unstable. This runtime option is controlled by namelist `nml_cgcm_recalc` and `nml_cgcm_recalc_replace`, which is explained in Tables 14.25 and 14.26.

Table14.25 Namelist `nml_cgcm_recalc`.

| variable name | units | description | usage |
|---|---|---|---|
| `l_recalc_flux` | logical | Recalculating of fluxes | default = `.false.` |

Table14.26 Namelist `nml_cgcm_recalc_replace`.

| variable name | units | description | usage |
|---|---|---|---|
| `l_recalc_replace_all` | logical | Replacing fluxes for all grid points | default = `.false.` |
| `file_recalc_replace` | character | File that contains mask that specify grid points where fluxes are replaced. | real(8) 2D array (1/0) written with direct access |

### 14.12.2 Properties of moist air

In MRI.COM, a set of formulae given by Gill (1982) is used to compute properties of moist air. Physical constants of sea water is listed on Table 2.1 of Chapter 2.

#### a. Saturation specific humidity

We consider computing saturation specific humidity in an environment with the sea surface temperature $t$ [°C] and the pressure $p$ [hPa].

The relation between the vapor pressure $e$ [hPa] and specific humidity $q$ is give by

$$e/p = q/(\epsilon + (1-\epsilon)q), \tag{14.120}$$

where $\epsilon$ is the molecular weight ratio between water vapor and air:

$$\epsilon = m_{\mathrm{w}}/m_{\mathrm{a}} = 18.016/28.966 = 0.62197. \tag{14.121}$$

This is solved for the specific humidity as

$$q = \epsilon e/(p - (1-\epsilon)e). \tag{14.122}$$

The relative humidity $\gamma$ is the ratio of the mixing ratio of the mass of vapor to the mass of dry air to the saturated one. The mixing ratio ($r$) of the mass of vapor to the mass of dry air is given by

$$r = \frac{q}{1-q}. \tag{14.123}$$

Thus the relative humidity is computed using the specific humidity $q$ and the saturation specific humidity $q_s$ as

$$\gamma = \frac{q(1-q_s)}{q_s(1-q)}. \tag{14.124}$$

The saturation vapor pressure $e_{sw}$ [hPa] of pure water vapor over a plane water surface is given by

$$\log_{10} e_{sw}(t) = (0.7859 + 0.03477\,t)/(1 + 0.00412\,t), \tag{14.125}$$

where $t$ is temperature between ±40 °C.

In air, the partial pressure $e'_{sw}$ of water vapor at saturation is not exactly $e_{sw}$ but is given by

$$e'_{sw} = f_w\, e_{sw}. \tag{14.126}$$

The value of $f_w$ is given by

$$f_w = 1 + 10^{-6} p(4.5 + 0.0006\,t^2), \tag{14.127}$$

where $p$ is the pressure (in units [hPa]).

The saturation vapor pressure over a salt solution is less than over fresh water. For sea water, the reduction is about 2 % (a factor of 0.98 should be applied to $e'_{sw}$).

The saturation vapor pressure $e_{si}$ of pure water vapor over ice is given by

$$\log_{10} e_{si}(t) = \log_{10} e_{sw}(t) + 0.00422\, t. \tag{14.128}$$

The saturation partial pressure $e'_{si}$ in moist air is $f_i$ times $e_{si}$. Values of $f_i$ are given correct to 1 part in $10^4$ by (14.127). Thus

$$e'_{si} = f_w\, e_{si}. \tag{14.129}$$

### b. Specific heat of air

$$\begin{aligned} c_{pa} &= \frac{7}{2} R\left(1 - q + \frac{8q}{7\epsilon}\right) \\ &= 1004.6 \times (1 + 0.8735q)\,\mathrm{J\,kg^{-1}\,K^{-1}} \end{aligned} \tag{14.130}$$

### c. Latent heat

The latent heat of vaporization is given by

$$L_v = 2.5008 \times 10^6 - 2.3 \times 10^3 t\,\mathrm{J\,kg^{-1}}. \tag{14.131}$$

The latent heat of sublimation is given by

$$L_s = 2.839 \times 10^6 - 3.6(t + 35)^2\,\mathrm{J\,kg^{-1}}. \tag{14.132}$$

### d. Air density ($\rho_a$)

The equation of state of moist air of temperature $T$ [K] under the pressure $P$ [Pa] is given by

$$\rho_a = \frac{P}{RT(1 - q + q/\epsilon)} \equiv P/RT_v, \tag{14.133}$$

where

$$T_v \equiv T(1 - q + q/\epsilon) = T(1 + c_{vt} q) \tag{14.134}$$

is called the virtual temperature,

$$c_{vt} = \frac{1}{\epsilon} - 1 = \frac{m_\mathrm{a}}{m_\mathrm{w}} - 1 \sim 0.6078, \tag{14.135}$$

and

$$R = 287.04\,\mathrm{J\,kg^{-1}\,K^{-1}} \tag{14.136}$$

is the gas constant of dry air.

# Chapter 15

# Turbulence Closure Models

The surface boundary layer is made turbulent by wind injecting momentum, so vertical mixing may be induced even if the stratification is stable. The stratification near the surface may be made gravitationally unstable by the surface buoyancy loss, so the vertical convection may be induced. Though these phenomena occur in small scales, they are important for the large scale oceanic processes. However, these are neither expressed by the fundamental equation of the general circulation models*, nor resolved by large scale models. Therefore, general circulation models express the effects of small scale turbulence by making some closure assumptions called turbulence closure in which mixing is expressed by synoptic states (velocity and temperature (salinity) solution of the model).

There are mainly two approaches to the turbulence closure problem: statistical closure models and empirical approaches. MRI.COM provides several options of statistical closure models, which are explained in this chapter. Note that an empirical approach of K-profile parameterization proposed by Large et al. (1994) is most popular in the ocean-climate modeling community. However, the current version of MRI.COM does not take this approach. In a future version, an interface to the Community Vertical Mixing Project (CVMix; Griffies et al., 2015) will be implemented to test the empirical approaches.

Three statistical turbulence closure models are supported: So called Mellor-Yamada model (Mellor and Yamada 1982, Mellor and Blumberg 2004) presented in Section 15.2, Noh and Kim (1999) model presented in Section 15.3, and a two-equation turbulence closure model using generic length-scale (GLS) equation by Umlauf and Burchard (2003) presented in Section 15.4. Table 15.1 summarizes features of turbulence closure models.

Table15.1 Features and equation numbers of turbulence closure models explained in this chapter.

| | Mellor and Yamada | Noh and Kim | Umlauf and Burchard |
|---|---|---|---|
| model option | `MELYAM` | `NOHKIM` | `GLS` |
| prognosticated variables | $q^2/2$ (15.42) | $E$(15.57) | $E$ (15.83), $\Psi$ (15.84) |
| surface boundary condition for TKE | specified (15.45) | flux (15.61) | flux (15.93) |
| formula for the length scale | (15.49), (15.48) | (15.75) | (15.78) |
| stability function | Solution of (15.39) | (15.72), (15.73) | (15.99), (15.100) |

## 15.1 Statistical closure model

In the statistical closure models, the physical properties in the basic equations of motion for a Boussinesq fluid are separated into averaged components and perturbed components (Reynolds decomposition), and then the equations are time averaged. The expressions for averaged velocity $\boldsymbol{U}$, averaged pressure $P$, and averaged potential temperature $\Theta$ are

$$\frac{\partial U_i}{\partial x_i} = 0, \tag{15.1}$$

$$\frac{DU_j}{Dt} + \epsilon_{jkl} f_k U_l = \frac{\partial}{\partial x_k}(-\langle u_k u_j \rangle) - \frac{1}{\rho_0}\frac{\partial P}{\partial x_j} - g_j \frac{\rho}{\rho_0} + \frac{\partial}{\partial x_k}\left[2\nu \frac{1}{2}\left(\frac{\partial U_k}{\partial x_j} + \frac{\partial U_j}{\partial x_k}\right)\right], \tag{15.2}$$

$$\frac{D\Theta}{Dt} = \frac{\partial}{\partial x_k}(-\langle u_k \theta \rangle) + \frac{\partial}{\partial x_k}\left(\kappa \frac{\partial \Theta}{\partial x_k}\right), \tag{15.3}$$

where $D(\ )/Dt \equiv U_k \partial(\ )/\partial x_k + \partial(\ )/\partial t$, $g_j$ is the gravity vector, $f_k$ is the Coriolis vector, $\epsilon_{ijk}$ is the alternating tensor, $\nu$ is viscosity, and $\kappa$ is diffusivity. Averaged quantities (resolved by the general circulation model) are represented by capital letters, and turbulent components (unresolved by the general circulation model) are represented by lower-case

* It could be expressed by relaxing the hydrostatic approximation but this is for future work.

letters. The statistical averages of the turbulent components are represented by $\langle\ \rangle$. The equation for salinity is similar to that for temperature (15.3). If density is calculated from temperature and salinity, the whole expression would become complicated. Therefore, density is assumed to be a function only of temperature here (we set $\rho = \beta\theta$, where $\beta$ is the coefficient of thermal expansion). Though these equations basically correspond to the MRI.COM governing equations (2.16)-(2.20), they now have contributions from subgrid-scale processes ($\langle u_k u_j \rangle$ and $\langle u_k \theta \rangle$), which is the focus of this chapter.

The equations (15.1)-(15.3) show that the statistical averages of the turbulent components ($\langle u_k u_j \rangle$ and $\langle u_k \theta \rangle$), which are called as the *second order moments*, are necessary to calculate the evolution of large scale quantities. However, they are unknown and their evolution must be solved explicitly if we do not use a parameterization to presume them on the basis of the large scale quantities. Following Kantha and Clayson (2000), the equations for the second order moments are expressed as follows:

$$\begin{aligned}
&\frac{D\langle u_i u_j\rangle}{Dt} + \frac{\partial}{\partial x_k}\left[\langle u_k u_i u_j\rangle - \nu\frac{\partial\langle u_i u_j\rangle}{\partial x_k}\right] + \frac{1}{\rho_0}\left[\frac{\partial\langle p u_i\rangle}{\partial x_j} + \frac{\partial\langle p u_j\rangle}{\partial x_i}\right] + f_k(\epsilon_{jkl}\langle u_l u_i\rangle + \epsilon_{ikl}\langle u_l u_j\rangle) \\
&\qquad = \left[-\langle u_k u_i\rangle\frac{\partial U_j}{\partial x_k} - \langle u_k u_j\rangle\frac{\partial U_i}{\partial x_k}\right] - \frac{\beta}{\rho_0}(g_j\langle u_i\theta\rangle + g_i\langle u_j\theta\rangle) + \left\langle\frac{p}{\rho_0}\left(\frac{\partial u_i}{\partial x_j} + \frac{\partial u_j}{\partial x_i}\right)\right\rangle - 2\nu\left\langle\frac{\partial u_i}{\partial x_k}\frac{\partial u_j}{\partial x_k}\right\rangle, \qquad (15.4)\\
&\frac{D\langle u_j\theta\rangle}{Dt} + \frac{\partial}{\partial x_k}\left[\langle u_k u_j\theta\rangle - \kappa\left\langle u_j\frac{\partial\theta}{\partial x_k}\right\rangle - \nu\left\langle\theta\frac{\partial u_j}{\partial x_k}\right\rangle\right] + \frac{1}{\rho_0}\left\langle\theta\frac{\partial p}{\partial x_j}\right\rangle + \epsilon_{jkl}f_k\langle u_l\theta\rangle \\
&\qquad = \left[-\langle u_j u_k\rangle\frac{\partial\Theta}{\partial x_k} - \langle u_k\theta\rangle\frac{\partial U_j}{\partial x_k}\right] - \frac{\beta}{\rho_0}g_j\langle\theta^2\rangle - (\kappa+\nu)\left\langle\frac{\partial u_j}{\partial x_k}\frac{\partial\theta}{\partial x_k}\right\rangle, \qquad (15.5)\\
&\frac{D\langle\theta^2\rangle}{Dt} + \frac{\partial}{\partial x_k}\left[\langle u_k\theta^2\rangle - \kappa\left\langle\frac{\partial\theta^2}{\partial x_k}\right\rangle\right] = -2\langle u_k\theta\rangle\frac{\partial\Theta}{\partial x_k} - 2\kappa\left\langle\frac{\partial\theta}{\partial x_k}\frac{\partial\theta}{\partial x_k}\right\rangle. \qquad (15.6)
\end{aligned}$$

Thus, to solve the evolution of the second order moments, information about higher moments such as $\langle uuu\rangle$, $\langle uu\theta\rangle$, $\langle u\theta^2\rangle$ is necessary. The system of equations is not closed, and assumption must be made at some level to close the problem.

The expression closed in the second order of the turbulent components is named second moment closure and is frequently used in modeling turbulence. Many models have been proposed to parameterize the higher order correlation terms in (15.4) through (15.6) in order to close the problem at the second moment. Those models differ mainly in the manner how the pressure-strain correlators are parameterized (Burchard and Bolding, 2001). After applying independent parameterizations for the higher order terms, the majority of models adopt several similar simplifications such as algebraization and boundary layer approximation that result in the "stability functions" of their own. Stability functions are determined by local shear and stability and relate the vertical gradient of large scale fields with vertical turbulent fluxes. Procedures adopted by major statistical closure models are summarized and compared by Burchard and Bolding (2001).

## 15.2 Mellor and Yamada model

Mellor and Yamada (1982) model is a classic model as well as a milestone in the efforts of finding practical solutions for marine and atmospheric boundary layers. We show some details of the simplifying procedures made in this model as a typical example. This is also intended to be an introduction to the problem of turbulence closure. However, it should be noted that this is neither unique nor final solution.

### 15.2.1 Fundamental closure assumptions

Mellor and Yamada (1982) closed the system (15.1)-(15.6) by reducing the higher order terms as follows. Based on Rotta's (1951a,1951b) hypothesis of energy redistribution, the covariances of pressure and velocity gradients are assumed to be linear functions of Reynolds stress:

$$\left\langle\frac{p}{\rho_0}\left(\frac{\partial u_i}{\partial x_j} + \frac{\partial u_j}{\partial x_i}\right)\right\rangle = -\frac{q}{3l_1}\left(\langle u_i u_j\rangle - \frac{\delta_{ij}}{3}q^2\right) + C_1 q^2\left(\frac{\partial U_i}{\partial x_j} + \frac{\partial U_j}{\partial x_i}\right), \qquad (15.7)$$

where $q^2 \equiv \langle u_i^2\rangle$, $l_1$ is the length scale, $C_1$ is a non-dimensional constant, and $\delta_{ij}$ is Kronecker's delta, which is unity for $i = j$ and zero for $i \neq j$.

Using Kolmogorov's hypothesis of local isotropy in small eddies, the energy dissipation is modeled as follows:

$$2\nu\left\langle\frac{\partial u_i}{\partial x_k}\frac{\partial u_j}{\partial x_k}\right\rangle = -\frac{2}{3}\frac{q^3}{\Lambda_1}\delta_{ij}, \qquad (15.8)$$

where $\Lambda_1$ is the length scale.

The redistribution of temperature and the dissipation of heat are modeled in the same form as above:

$$\left\langle \frac{p}{\rho_0}\frac{\partial\theta}{\partial x_j}\right\rangle = -\frac{q}{3l_2}\langle u_j\theta\rangle \tag{15.9}$$

$$(\kappa+\nu)\left\langle \frac{\partial u_j}{\partial x_k}\frac{\partial\theta}{\partial x_k}\right\rangle = 0, \tag{15.10}$$

where $l_2$ is the length scale. The dissipation of temperature variance is

$$2\kappa\left\langle \frac{\partial\theta}{\partial x_k}\frac{\partial\theta}{\partial x_k}\right\rangle = -2\frac{q}{\Lambda_2}\langle\theta^2\rangle, \tag{15.11}$$

where $\Lambda_2$ is the length scale.

In order to avoid the higher order problems, the turbulent velocity diffusion term and the other higher order terms are modeled as follows:

$$\langle u_k u_i u_j\rangle = \frac{3}{5}lqS_q\left(\frac{\partial\langle u_i u_j\rangle}{\partial x_k}+\frac{\partial\langle u_i u_k\rangle}{\partial x_j}+\frac{\partial\langle u_j u_k\rangle}{\partial x_i}\right), \tag{15.12}$$

$$\langle u_k u_j\theta\rangle = -lqS_{u\theta}\left(\frac{\partial\langle u_k\theta\rangle}{\partial x_j}+\frac{\partial\langle u_j\theta\rangle}{\partial x_k}\right), \tag{15.13}$$

$$\langle u_k\theta^2\rangle = -lqS_\theta\frac{\partial\langle\theta^2\rangle}{\partial x_k}, \tag{15.14}$$

where $S_q$, $S_{u\theta}$, and $S_\theta$ are non-dimensional numbers and can be set as constants or functions of certain parameters. Other relations are $\langle p\theta\rangle = 0$ and $\langle pu_i\rangle = 0$.

The essence of the Mellor-Yamada mixed layer model is that the above length scales are related linearly to each other:

$$(l_1,\Lambda_1,l_2,\Lambda_2) = (A_1,B_1,A_2,B_2)l, \tag{15.15}$$

where $l$ is the vertical scale of turbulence (also called the master length scale), and $A_1, B_1, A_2, B_2$, and $C_1$ are empirical constants and are determined from experiment data. Mellor and Yamada (1982) employ $(A_1,B_1,A_2,B_2,C_1) = (0.92, 16.6, 0.74, 10.1, 0.08)$.

### 15.2.2 Algebraization, boundary layer approximation, and stability functions for the level 2.5 model

The turbulence model that solves the evolution of the statistically averaged values of the second-order turbulent components based on the simplification described in the previous subsection is called the level-4 model.

The level-3 model solves the evolution of the turbulent kinetic energy ($q^2/2$) and the variance of potential temperature ($\langle\theta^2\rangle$) (in some cases, the covariance of potential temperature and salinity ($\langle\theta s\rangle$) and the variance of salinity ($\langle s^2\rangle$)). The other statistically averaged values are solved diagnostically through algebraic equations assuming them to be in the steady state.

In the level-2.5 model, the variance of the potential temperature is also assumed to be in a statistically steady state (see expression (15.33) that appears later).

In the level-2 model, the turbulent kinetic energy is also assumed to be in a statistically steady state.

The level-2.5 model, which is employed as a surface boundary layer model by MRI.COM, is further simplified by applying the following boundary layer approximations.

- Neglect the Coriolis term in the equations of motion for the turbulent components.
- Neglect the molecular viscosity and diffusivity.
- Use the hydrostatic assumption in the vertical component of the equation of motion.
- Consider only vertical differentiation (direction perpendicular to the boundary) in the spatial differentiation for the term involving turbulent velocity.

The equations for the large scale quantities, (15.2) and (15.3), become

$$\frac{DU}{Dt} + \frac{\partial}{\partial z}\langle uw\rangle = -\frac{1}{\rho_0}\frac{\partial P}{\partial x} + fV, \tag{15.16}$$

$$\frac{DV}{Dt} + \frac{\partial}{\partial z}\langle vw\rangle = -\frac{1}{\rho_0}\frac{\partial P}{\partial y} - fU, \tag{15.17}$$

$$0 = -\frac{1}{\rho_0}\frac{\partial P}{\partial z} - g\frac{\rho}{\rho_0}, \tag{15.18}$$

$$\frac{D\Theta}{Dt} + \frac{\partial}{\partial z}(\langle w\theta\rangle) = \frac{1}{\rho_0 c_p}\frac{\partial R}{\partial z}. \tag{15.19}$$

In (15.19), $R$ is the heat flux due to penetration of shortwave radiation. The level-2.5 system consists of the time evolution equation for turbulent kinetic energy and algebraic equations for other second-moment turbulent quantities.

The time evolution equation for the turbulent kinetic energy is

$$\frac{D}{Dt}\left(\frac{q^2}{2}\right) - \frac{\partial}{\partial z}\left[lqS_q\frac{\partial}{\partial z}\left(\frac{q^2}{2}\right)\right] = P_s + P_b - \epsilon, \tag{15.20}$$

where

$$P_s = -\langle wu\rangle\frac{\partial U}{\partial z} - \langle wv\rangle\frac{\partial V}{\partial z} \tag{15.21}$$

is the term for energy produced by the vertical shear of the averaged flow,

$$P_b = -g\langle w\rho\rangle/\rho_0 \tag{15.22}$$

is the term for energy produced by buoyancy, and

$$\epsilon = q^3/\Lambda_1 \tag{15.23}$$

is the energy dissipation term. The constant $S_q$ is given in the next subsection.

The algebraic equations for the statistically averaged values, which are expressed by other second-moment turbulent quantities, are given below.

$$\langle u^2\rangle = \frac{q^2}{3} + \frac{l_1}{q}\left[-4\langle wu\rangle\frac{\partial U}{\partial z} + 2\langle wv\rangle\frac{\partial V}{\partial z} - 2P_b\right], \tag{15.24}$$

$$\langle v^2\rangle = \frac{q^2}{3} + \frac{l_1}{q}\left[2\langle wu\rangle\frac{\partial U}{\partial z} - 4\langle wv\rangle\frac{\partial V}{\partial z} - 2P_b\right], \tag{15.25}$$

$$\langle w^2\rangle = \frac{q^2}{3} + \frac{l_1}{q}\left[2\langle wu\rangle\frac{\partial U}{\partial z} + 2\langle wv\rangle\frac{\partial V}{\partial z} + 4P_b\right], \tag{15.26}$$

$$\langle uv\rangle = \frac{3l_1}{q}\left[-\langle uw\rangle\frac{\partial V}{\partial z} - \langle vw\rangle\frac{\partial U}{\partial z}\right], \tag{15.27}$$

$$\langle wu\rangle = \frac{3l_1}{q}\left[-(\langle w^2\rangle - C_1q^2)\frac{\partial U}{\partial z} - g\langle u\rho\rangle\right], \tag{15.28}$$

$$\langle vw\rangle = \frac{3l_1}{q}\left[-(\langle w^2\rangle - C_1q^2)\frac{\partial V}{\partial z} - g\langle v\rho\rangle\right], \tag{15.29}$$

$$\langle u\theta\rangle = \frac{3l_2}{q}\left[-\langle uw\rangle\frac{\partial\Theta}{\partial z} - \langle w\theta\rangle\frac{\partial U}{\partial z}\right], \tag{15.30}$$

$$\langle v\theta\rangle = \frac{3l_2}{q}\left[-\langle vw\rangle\frac{\partial\Theta}{\partial z} - \langle w\theta\rangle\frac{\partial V}{\partial z}\right], \tag{15.31}$$

$$\langle w\theta\rangle = \frac{3l_2}{q}\left[-\langle w^2\rangle\frac{\partial\Theta}{\partial z} - g\langle\theta\rho\rangle\right], \tag{15.32}$$

$$\langle\theta^2\rangle = -\frac{\Lambda_2}{q}\langle w\theta\rangle\frac{\partial\Theta}{\partial z}. \tag{15.33}$$

Some of the terms in these equations, which are used in (15.16)-(15.19), can be further deformed by substitution as

follows:

$$-\langle uw\rangle = K_M \frac{\partial U}{\partial z}, \tag{15.34}$$

$$-\langle vw\rangle = K_M \frac{\partial V}{\partial z}, \tag{15.35}$$

$$-\langle \theta w\rangle = K_H \frac{\partial \Theta}{\partial z}, \tag{15.36}$$

$$K_M = lqS_M, \tag{15.37}$$

$$K_H = lqS_H. \tag{15.38}$$

This simplification means that the vertical turbulent fluxes are proportional to the gradient of the large scale fields. The ultimate purpose of solving the mixed layer model is to determine the coefficients of momentum and heat fluxes, $K_M$ and $K_H$, using (15.37) and (15.38).

Assuming that the potential density is linearly related to the potential temperature (and salinity), the simultaneous equations for $S_M$ and $S_H$ are derived as follows:

$$\begin{aligned} S_M[6A_1A_2g_M] + S_H[1 - 3A_2B_2g_H - 12A_1A_2g_H] &= A_2, \\ S_M[1 + 6A_1^2g_M - 9A_1A_2g_H] - S_H[12A_1^2g_H + 9A_1A_2g_H] &= A_1(1 - 3C_1), \end{aligned} \tag{15.39}$$

where

$$g_M \equiv \frac{l^2}{q^2}\left[\left(\frac{\partial U}{\partial z}\right)^2 + \left(\frac{\partial V}{\partial z}\right)^2\right] = \frac{l^2}{q^2}S^2, \tag{15.40}$$

$$g_H \equiv -\frac{l^2}{q^2}\frac{g}{\rho_0}\frac{\partial \tilde{\rho}}{\partial z} = \frac{l^2}{q^2}N^2, \tag{15.41}$$

and $\partial\tilde{\rho}/\partial z$ is the vertical gradient of potential density. Note that $S_M$ and $S_H$ are stability functions of this closure model.

Using $S_M$ and $S_H$, $K_M$ and $K_H$ are then obtained from (15.37) and (15.38) by determining $q$ and $l$.

### 15.2.3 Solving for velocity scale ($q$) and length scale ($l$)

The turbulent velocity $q$ is obtained by solving the following expression that is modified from (15.20) using the above results:

$$\frac{\partial}{\partial t}\left(\frac{q^2}{2}\right) - \frac{\partial}{\partial z}\left[K_E\frac{\partial}{\partial z}\left(\frac{q^2}{2}\right)\right] = K_M\left[\left(\frac{\partial U}{\partial z}\right)^2 + \left(\frac{\partial V}{\partial z}\right)^2\right] + \frac{g}{\rho_0}K_H\frac{\partial \tilde{\rho}}{\partial z} - \epsilon, \tag{15.42}$$

where

$$K_E = lqS_q \tag{15.43}$$

and advection terms are neglected. In MRI.COM, $S_q$ is set proportional to $S_M$ ($S_q \propto S_M$). We adopt the form $S_q = S_{qc}S_M/S_{Mn}$, where $S_{qc} = 0.2$ and $S_{Mn} = 0.3927$. With this choice, $S_q = 0.2$ when the stratification is neutral ($g_H = 0$).

The sea surface boundary condition for the turbulent kinetic energy follows Mellor and Blumberg (2004):

$$K_q\frac{\partial q^2}{\partial z} = 2\alpha_{\mathrm{CB}}u_\tau^3, \tag{15.44}$$

where $\alpha_{\mathrm{CB}} = 100$ and $u_\tau$ is the frictional velocity defined as $u_\tau \equiv (\tau_s/\rho_s)^{1/2}$ by using the surface stress ($\tau_s$) and the sea surface density ($\rho_s$). Mellor and Blumberg (2004) showed that this flux boundary condition is analytically converted to the condition for $q$ at the sea surface:

$$q^2 = (15.8\alpha_{\mathrm{CB}})^{2/3}u_\tau^2. \tag{15.45}$$

On the other hand, the bottom boundary condition is

$$q = 0. \tag{15.46}$$

The vertical scale of the turbulence (master length scale, $l$) is estimated by many formulae such as a time evolution equation (which is usually empirical and is not completely based on physics) and a diagnosis. MRI.COM uses different diagnosis equations for the surface layer influenced directly by surface wind wave effects and for the internal region. The

surface layer is defined by a depth of $|z| < z_w$, where the roughness parameter $z_w$ due to surface wind waves is given by Mellor and Blumberg (2004) as follows:

$$z_w = \beta_w \frac{u_\tau^2}{g}, \qquad \beta_w = 2.0 \times 10^5. \tag{15.47}$$

In this layer, the formula for $l$ is

$$l = \kappa z_w, \tag{15.48}$$

where $\kappa$ is the von Karman constant ($\kappa = 0.4$). In the internal region ($|z| > z_w$), the formula for $l$ is

$$l = \gamma \int_{z_b}^{0} |z'| q dz' \Big/ \int_{z_b}^{0} q dz', \tag{15.49}$$

where $\gamma = 0.2$, and $z_b$ is the water depth. This is recognized as the averaged depth with the weight of the kinetic energy, which is sufficient for the ocean boundary layer according to Mellor and Yamada (1982).

### 15.2.4 Implementation

This section briefly describes the solution procedure.

The mixed layer model (subroutine name `mysl25` in `my25.F90`) is called as the last procedure of each time step that proceeds from n to n+1. After the master length scale ($l$) for the present time step (n) is determined using (15.48) and (15.49), where the latter is actually computed in the previous time step, the turbulent kinetic energy ($q^2/2$) is solved using (15.42) with (15.23) under the boundary conditions of (15.45) and (15.46), where the forward finite difference (n $\longrightarrow$ n+1) is used in time. The implicit method is used for the vertical diffusion of the turbulent kinetic energy and energy dissipation term, since these terms could become significantly large (see Section 23.5). The vertical viscosity and diffusivity for the time step n+1 are estimated using $q$, $l$, and (15.37) to (15.39). These are used in the governing equations for the synoptic scale field. The vertical scale of the turbulence (master length scale) based on the turbulence kinetic energy (15.49) is calculated to prepare for the next time step.

The turbulent kinetic energy and the master length scale are defined at the bottom of the tracer cell $(i, j, k)$. The specific expression for the discretized form of the turbulent kinetic energy ($E = q^2/2$) equation, (15.42), is as follows:

$$\begin{aligned}
\frac{E_k^{n+1} - E_k^n}{\Delta t} =& \frac{1}{\Delta z_k}\left[\frac{K_{E\,k-\frac{1}{2}}(E_{k-1}^{n+1} - E_k^{n+1})}{\Delta z_{k-\frac{1}{2}}} - \frac{K_{E\,k+\frac{1}{2}}(E_k^{n+1} - E_{k+1}^{n+1})}{\Delta z_{k+\frac{1}{2}}}\right] \\
&+ K_{M\,k}\frac{(U_{k-\frac{1}{2}}^{n+1} - U_{k+\frac{1}{2}}^{n+1})(\tilde{U}_{k-\frac{1}{2}} - \tilde{U}_{k+\frac{1}{2}})}{\Delta z_k^2} + K_{M\,k}\frac{(V_{k-\frac{1}{2}}^{n+1} - V_{k+\frac{1}{2}}^{n+1})(\tilde{V}_{k-\frac{1}{2}} - \tilde{V}_{k+\frac{1}{2}})}{\Delta z_k^2} \\
&- K_{H\,k}\frac{B_{k-\frac{1}{2}}^{n+1} - B_{k+\frac{1}{2}}^{n+1}}{\Delta z_k} - 2E_k^{n+1} q_k^n / B_1 l_k^n,
\end{aligned} \tag{15.50}$$

where $\tilde{U} = (U^{n+1} + U^n)/2$, $\tilde{V} = (V^{n+1} + V^n)/2$, and $B$ is buoyancy ($= -\frac{g\rho}{\rho_0}$). The discrete expression for shear production (the second and third terms on the r.h.s.) and the buoyancy sink (the fourth term on the r.h.s.) follows Burchard (2002), which is consistent with the conservation law of the sum of mean and turbulent energy.

To summarize, the numerical operations proceed in the following order:

1. Calculate the master length scale for the present time step using (15.47) and (15.48) as well as (15.49) from the previous time step.
2. Update the turbulent kinetic energy using (15.50), (15.45) and (15.46).
3. Solve the algebraic equation for $S_M$ and $S_H$ using (15.39).
4. Calculate the vertical viscosity and diffusivity for the next time step using (15.37), (15.38), and (15.43).
5. Calculate the master length scale using (15.49) in preparation for the next time step.

### 15.2.5 Usage

Mellor and Yamada model is invoked by `MELYAM` option on compilation. There is no tuning parameter at run time. Initial state for vertical diffusion of turbulence kinetic energy ($K_E$), turbulence kinetic energy ($q$), and length scale ($l$) is read from restart file. Otherwise it is set as a state without turbulence. The state without turbulence is zero turbulence kinetic energy ($q = 0$), the mixing length of 1 meter ($l = 1$ m) and the vertical diffusion of turbulence kinetic energy is the constant

background vertical viscosity given by `visc_vert_bg_cm2ps` in namelist `nml_visc_vert_bg`. How model is initialized is specified by namelist `nml_melyam_run`. Parameters are listed on Table 15.2.

Table15.2 namelist `nml_melyam_run`

| variable name | units | description | usage |
|---|---|---|---|
| `l_rst_melyam_in` | logical | `.true.` : Read restart files specified by `nmlrs_my_avq`, `nmlrs_my_q`, and `nmlrs_my_alo` for the initial condition.<br>`.false.`: Start condition is that of no turbulence. See text for details. | default = `l_rst_in` of `nml_run_ini_state` |

## 15.3 Noh and Kim (1999) model

The mixed layer model proposed by Mellor and Yamada was originally developed for the atmospheric boundary layer, and its surface boundary is treated as a solid wall. When they applied this model to the ocean, they regarded that the turbulent kinetic energy is injected into the ocean by the wind stress at the solid-wall sea surface. The model by Mellor and Yamada could therefore be considered to insufficiently represent the oceanic turbulent mixed layer.

Noh and Kim (1999) presented a model that can resolve this insufficiency. The model is basically the same as Mellor and Yamada level 2.5 scheme in that turbulent kinetic energy is prognosticated and the length scale is diagnostically determined. It differs in the stability function and the treatment of surface boundary condition.

### 15.3.1 Fundamental equation

The equations for the zonal and meridional components of the velocity, $U$, $V$, buoyancy $B = -g\Delta\rho/\rho_0$, and turbulent energy $E$ in the large scale fields are

$$\frac{DU}{Dt} = -\frac{\partial}{\partial z}\langle uw\rangle - \frac{1}{\rho_0}\frac{\partial P}{\partial x} + fV, \tag{15.51}$$

$$\frac{DV}{Dt} = -\frac{\partial}{\partial z}\langle vw\rangle - \frac{1}{\rho_0}\frac{\partial P}{\partial y} - fU, \tag{15.52}$$

$$\frac{DB}{Dt} = -\frac{\partial}{\partial z}\langle bw\rangle + \frac{\partial R}{\partial z}, \tag{15.53}$$

$$\frac{DE}{Dt} = -\frac{\partial}{\partial z}\left\langle w\left(\frac{p}{\rho_0} + uu + vv + ww\right)\right\rangle - \langle uw\rangle\frac{\partial U}{\partial z} - \langle vw\rangle\frac{\partial V}{\partial z} + \langle bw\rangle - \epsilon, \tag{15.54}$$

where $R$ is the downward shortwave radiation and $\partial R/\partial z$ is its convergence.

The turbulent flux is expressed by using the large scale fields (in capital letters) as follows:

$$\frac{DU}{Dt} = \frac{\partial}{\partial z}\left(K_M\frac{\partial U}{\partial z}\right) - \frac{1}{\rho_0}\frac{\partial P}{\partial x} + fV, \tag{15.55}$$

$$\frac{DV}{Dt} = \frac{\partial}{\partial z}\left(K_M\frac{\partial V}{\partial z}\right) - \frac{1}{\rho_0}\frac{\partial P}{\partial y} - fU, \tag{15.56}$$

$$\frac{DB}{Dt} = \frac{\partial}{\partial z}\left(K_H\frac{\partial B}{\partial z}\right) - \frac{\partial R}{\partial z}, \tag{15.57}$$

$$\frac{DE}{Dt} = \frac{\partial}{\partial z}\left(K_E\frac{\partial E}{\partial z}\right) + K_M\frac{\partial U}{\partial z}\frac{\partial U}{\partial z} + K_M\frac{\partial V}{\partial z}\frac{\partial V}{\partial z} - \left(K_H\frac{\partial B}{\partial z}\right) - \epsilon. \tag{15.58}$$

The surface boundary conditions are as follows:

$$K_M\frac{\partial U}{\partial z} = \frac{\tau}{\rho_0}, \tag{15.59}$$

$$K_H\frac{\partial B}{\partial z} = Q_0, \tag{15.60}$$

$$K_E\frac{\partial E}{\partial z} = mu_\tau^3, \tag{15.61}$$

where $m$ is a tuning parameter and $m = 100$ is recommended by Noh and Kim (1999). Unlike Mellor and Yamada model, a flux boundary condition is used for turbulence kinetic energy. This is intended to express the direct input of turbulence kinetic energy due to wind waves. As such, in the presence of sea ice, the direct input of wave energy may be more appropriate only through open water. The boundary condition may be optionally modified so that

$$K_E \frac{\partial E}{\partial z} = m u_\tau^3 (1 - a), \tag{15.62}$$

where $a$ is area fraction of sea ice. The no-flux condition is used for the bottom:

$$K_E \frac{\partial E}{\partial z} = 0. \tag{15.63}$$

### 15.3.2 Stability function

The central problem is how to determine the viscosity, diffusivity ($K_M, K_H, K_E$), and turbulent energy dissipation rate ($\epsilon$). In the Noh and Kim (1999) scheme, by using the typical velocity scale ($q = (2E)^{1/2}$) and the vertical length scale ($l$) of the turbulence, they are obtained by the following formula:

$$K_M = Sql, \tag{15.64}$$
$$K_H = S_B ql, \tag{15.65}$$
$$K_E = S_E ql, \tag{15.66}$$
$$\epsilon = Cq^3 l^{-1}. \tag{15.67}$$

The constants ($S, S_B, S_E, C$) are obtained from experiments. For neutral stratification, it is assumed that $S = 0.39$, $Pr \equiv S/S_B = 0.8$, $\sigma \equiv S/S_E = 1.95$, and $C = 0.06$. Hereafter, these values for neutral stratification are denoted as $S_0$, $Pr_0$, $\sigma_0$, and $C_0$, respectively.

Regarding the influence of the stratification, that is, stability function, we assume that the vertical scale of turbulence is limited by the vertical scale of buoyancy $l_b = q/N$ ($N^2 = \partial B/\partial z$). That is,

$$K \sim q l_b \sim q l \mathrm{Ri}_t^{-1/2}, \tag{15.68}$$

where $\mathrm{Ri}_t$ is the turbulent Richardson number

$$\mathrm{Ri}_t = (Nl/q)^2. \tag{15.69}$$

$\mathrm{Ri}_t$ corresponds to $g_H$ of Mellor and Yamada model. See (15.41).

This means that when the stratification is strong ($N$ is large, $\mathrm{Ri}_t$ is large, and $K$ is small), the turbulent energy is not transported downwards. It could also be considered that the local turbulent energy dissipation becomes large.

The following equation is used for $S$ so that it satisfies (15.68) when $\mathrm{Ri}_t$ is large:

$$S/S_0 = (1 + \alpha \mathrm{Ri}_t)^{-1/2}, \tag{15.70}$$

where $\alpha$ is a tuning parameter. Noh and Kim (1999) recommend $\alpha \sim 120.0$, but $\alpha \sim 5.0$ is the default value of MRI.COM.

The effect of stratification on the Prandtl number ($Pr$) is set following Noh et al. (2005):

$$Pr/Pr_0 = (1 + \beta \mathrm{Ri}_t)^{1/2}, \tag{15.71}$$

where $\beta$ is a tuning parameter and 0.5 is used following Noh et al. (2005).

To summarize, the stability function for this model is expressed as follows:

$$S = \frac{S_0}{(1 + \alpha \mathrm{Ri}_t)^{1/2}} \tag{15.72}$$
$$S_B = \frac{S}{Pr} = \frac{S_0}{Pr_0 (1 + \alpha \mathrm{Ri}_t)^{1/2} (1 + \beta \mathrm{Ri}_t)^{1/2}}. \tag{15.73}$$

The effect of stratification on the energy dissipation ($C$) is set as follows:

$$C/C_0 = (1 + \alpha \mathrm{Ri}_t)^{1/2}. \tag{15.74}$$

Note that this is independent of stratification for Mellor and Yamada and Umlauf and Burchard (2003) model.

In the case of unstable stratification ($N^2 < 0$), $K_M = K_H = 1.0\,\mathrm{m^2\,s^{-1}}$ and $K_E$ is estimated from the turbulent velocity scale and the vertical length scale in the model. This treatment is due to the difference between the time scales of the vertical convection and the development of turbulence.

Finally, the vertical scale of turbulence is diagnosed as

$$l = \frac{\kappa(|z| + z_0)}{(1 + \kappa(|z| + z_0)/h)}, \tag{15.75}$$

where $z_0$ is the sea surface roughness ($z_0 = 1$ m), $z$ is the depth, and $h$ is the mixed layer depth. The mixed layer depth ($h$) is determined as the depth at which the buoyancy frequency becomes the maximum in the vertical column. The vertical scale becomes longer as the mixed layer becomes deeper.

### 15.3.3 Implementation

Equation (15.58) is solved for the prognostic variable $E$ in the subroutine `nkoblm` in `nkoblm.F90` as the last procedure of each time step. The forward finite difference is used in the time evolution. The implicit method is used for the vertical diffusion of the turbulent kinetic energy and energy dissipation term, since these terms could become significantly large (see Section 23.5). The new $E$ is used to determine the coefficients of viscosity and diffusivity for the next time step.

The turbulent kinetic energy and the master length scale are defined at the center of the tracer cell $(i, j, k - \frac{1}{2})$. The specific expression for the discretized form of the turbulent kinetic energy ($E$) equation is as follows:

$$\begin{aligned}
\frac{E^{n+1}_{k-\frac{1}{2}} - E^{n}_{k-\frac{1}{2}}}{\Delta t} =& \frac{1}{\Delta z_{k-\frac{1}{2}}}\left[\frac{K_{E\,k-1}(E^{n+1}_{k-\frac{3}{2}} - E^{n+1}_{k-\frac{1}{2}})}{\Delta z_{k-1}} - \frac{K_{E\,k}(E^{n+1}_{k-\frac{1}{2}} - E^{n+1}_{k+\frac{1}{2}})}{\Delta z_k}\right] \\
&+ \frac{1}{2}K_{M\,k-1}\frac{(u^{n+1}_{k-\frac{3}{2}} - u^{n+1}_{k-\frac{1}{2}})(u^{n+1}_{k-\frac{3}{2}} - u^{n}_{k-\frac{1}{2}})}{\Delta z_{k-1}\Delta z_{k-\frac{1}{2}}} + \frac{1}{2}K_{M\,k}\frac{(u^{n+1}_{k-\frac{1}{2}} - u^{n+1}_{k+\frac{1}{2}})(u^{n}_{k-\frac{1}{2}} - u^{n+1}_{k+\frac{1}{2}})}{\Delta z_k\Delta z_{k-\frac{1}{2}}} \\
&+ \frac{1}{2}K_{M\,k-1}\frac{(v^{n+1}_{k-\frac{3}{2}} - v^{n+1}_{k-\frac{1}{2}})(v^{n+1}_{k-\frac{3}{2}} - v^{n}_{k-\frac{1}{2}})}{\Delta z_{k-1}\Delta z_{k-\frac{1}{2}}} + \frac{1}{2}K_{M\,k}\frac{(v^{n+1}_{k-\frac{1}{2}} - v^{n+1}_{k+\frac{1}{2}})(v^{n}_{k-\frac{1}{2}} - v^{n+1}_{k+\frac{1}{2}})}{\Delta z_k\Delta z_{k-\frac{1}{2}}} \\
&- \frac{1}{2}K_{H\,k-1}\frac{B^{n+1}_{k-\frac{3}{2}} - B^{n+1}_{k-\frac{1}{2}}}{\Delta z_{k-1}} - \frac{1}{2}K_{H\,k}\frac{B^{n+1}_{k-\frac{1}{2}} - B^{n+1}_{k+\frac{1}{2}}}{\Delta z_k} - 2CE^{n+1}_{k-\frac{1}{2}}q^{n}_{k-\frac{1}{2}}/l^{n}_{k-\frac{1}{2}}.
\end{aligned} \tag{15.76}$$

The discrete expression for the shear production (the second through fifth terms on the r.h.s.) and the buoyancy sink (the sixth term on the r.h.s.) follows Burchard (2002), which is consistent with the conservation law of the sum of mean and turbulent energy.

To summarize, the numerical operations proceed in the following order:

1. Update the master length scale using (15.75),
2. Update the turbulent kinetic energy using (15.76) under the boundary conditions (15.61) and (15.63)
3. Calculate the vertical viscosity and diffusivity for the next time step (15.64) and (15.65).

### 15.3.4 Usage

Noh and Kim (1999) model is invoked by `NOHKIM` option on compilation.

Initial state for vertical diffusion of turbulence kinetic energy ($K_E$), turbulence kinetic energy ($E$) is either read from restart file or set as a state without turbulence. The state without turbulence means that $E$ is very small as $\frac{1}{2}{q_{\min}}^2$, where $q_{\min} = 1 \times 10^{-5}\,\mathrm{m\,s^{-1}}$ is the minimum of turbulence velocity scale, and that $K_E$ is set the constant background vertical viscosity given by `visc_vert_bg_cm2ps` in namelist `nml_visc_vert_bg`. How model is initialized is specified by namelist `nml_nohkim_run`. Parameters are listed on Table 15.4.

Tuning parameters may be specified at run time by namelist `nml_nkoblm`. Parameters are listed on Table 15.3.

Table15.3 namelist `nml_nkoblm`

| variable name | units | description | usage |
|---|---|---|---|
| `mfnk` | 1 | $m$ of Eq. (15.61) | default = 100.0 |
| `alpnk` | 1 | $\alpha$ of Eq. (15.70) | default = 5.0 |
| `betank` | 1 | $\beta$ of Eq. (15.71) | default = 0.5 |
| `l_wave_damp_seaice` | logical | Eq. (15.62) is used instead of (15.61) | default = `.false.` |

Table15.4 namelist `nml_nohkim_run`

| variable name | units | description | usage |
|---|---|---|---|
| `l_rst_nohkim_in` | logical | `.true.` : Read restart files specified by `nmlrs_nk_avq` and `nmlrs_nk_eb` for the initial condition. `.false.`: Start condition is that of no turbulence. See text for details. | default = `l_rst_in` of `nml_run_ini_state` |

## 15.4 Generic length scale model by Umlauf and Burchard (2003)[†]

The turbulent closure models of Mellor and Yamada level 2.5 (section 15.2) and Noh and Kim (section 15.3) as incorporated in MRI.COM have only one prognostic variable of turbulence (turbulent kinetic energy). These may be classed as "one-equation" turbulent closure models. In these models, some formulae for length scale are given (e.g., (15.49) and (15.75)). Therefore the turbulent length scale $l$ is not a predicted but a diagnosed quantity.

Generic length scale model by Umlauf and Burchard (2003) is a generalized form of two-equation turbulence models. It introduces a generic length-scale variable $\psi$ as the second variable, expressed as

$$\psi = (c_\mu^0)^p E^m l^n. \tag{15.77}$$

With $E$ and $\psi$ given, the turbulent length scale can be computed as

$$l = (c_\mu^0)^{-\frac{p}{n}} E^{-\frac{m}{n}} \psi^{\frac{1}{n}}, \tag{15.78}$$

and the dissipation rate $\epsilon$ can be computed from the following relation,

$$\epsilon = (c_\mu^0)^3 \frac{E^{3/2}}{l}. \tag{15.79}$$

With appropriate values of the exponents $p$, $m$, $n$ in (15.77), a number of well-known two-equation models (e.g., $k$-$\epsilon$ model and $k$-$\omega$ model) can be identified as special case of the generic model.

### 15.4.1 Fundamental equation

The fundamental equations for $U$, $V$, $B$ and $E$ are basically common to those of Noh and Kim model. The equation for generic length scale variable $\psi$ is added. Expressing the turbulent flux using the large scale fields with the assumption of horizontally homogeneous flow, the fundamental equations of the model is expressed as follows:

$$\frac{DU}{Dt} = \frac{\partial}{\partial z}\left(K_M \frac{\partial U}{\partial z}\right) - \frac{1}{\rho_0}\frac{\partial P}{\partial x} + fV, \tag{15.80}$$

$$\frac{DV}{Dt} = \frac{\partial}{\partial z}\left(K_M \frac{\partial V}{\partial z}\right) - \frac{1}{\rho_0}\frac{\partial P}{\partial y} - fU, \tag{15.81}$$

$$\frac{DB}{Dt} = \frac{\partial}{\partial z}\left(K_H \frac{\partial B}{\partial z}\right) - \frac{\partial R}{\partial z}, \tag{15.82}$$

$$\frac{DE}{Dt} = \frac{\partial}{\partial z}\left(K_E \frac{\partial E}{\partial z}\right) + P_\mathrm{s} + P_\mathrm{b} - \epsilon, \tag{15.83}$$

$$\frac{D\psi}{Dt} = \frac{\partial}{\partial z}\left(K_\psi \frac{\partial \psi}{\partial z}\right) + \frac{\psi}{E}(c_{\psi 1} P_\mathrm{s} + c_{\psi 3} P_\mathrm{b} - c_{\psi 2}\epsilon), \tag{15.84}$$

[†] This model is implemented by Shiro Nishikawa as he was a visiting researcher at MRI.

where $P_s$ and $P_b$ are the shear production and the buoyancy production expressed according to

$$P_s = -\langle uw \rangle \frac{\partial u}{\partial z} - \langle vw \rangle \frac{\partial v}{\partial z} = K_M M^2, \qquad P_b = \langle bw \rangle = -K_H N^2, \tag{15.85}$$

and

$$M^2 = \left(\frac{\partial u}{\partial z}\right)^2 + \left(\frac{\partial v}{\partial z}\right)^2, \qquad N^2 = \frac{\partial B}{\partial z} \tag{15.86}$$

are the shear frequency and the buoyancy frequency, respectively. The vertical turbulent diffusivities in horizontally homogeneous flows are expressed as

$$K_M = c_\mu E^{1/2} l, \tag{15.87}$$

$$K_H = c'_\mu E^{1/2} l, \tag{15.88}$$

$$K_E = c_\mu E^{1/2} l / \sigma_k^\psi, \tag{15.89}$$

$$K_\psi = c_\mu E^{1/2} l / \sigma_\psi, \tag{15.90}$$

where $c_\mu$ and $c'_\mu$ are stability functions and $\sigma_k^\psi$ and $\sigma_\psi$ are the constant Schmidt numbers. Here, $c_\mu$ and $c'_\mu$ corresponds to $S_M$, and $S_H$ of the Mellor and Yamada model with a relation

$$c_\mu = \sqrt{2} S_M, \quad c'_\mu = \sqrt{2} S_H. \tag{15.91}$$

In the case of unstable stratification ($N^2 < 0$), $K_M = K_H = 1.0\,\mathrm{m^2\,s^{-1}}$ is used in MRI.COM. This treatment is common to Noh and Kim model (section 15.3).

### 15.4.2 Boundary conditions

At the surface, the shear-free boundary layers with injection of turbulent kinetic energy are assumed, in which

$$E = K(-z + z_0)^\alpha, \quad l = L(-z + z_0), \tag{15.92}$$

are supposed, where $K$ is the scale of turbulent kinetic energy, $L$ and $\alpha$ are empirical constants given in Table 15.5, and $z_0$ is the sea surface roughness ($z_0 = 1\,\mathrm{m}$). $K$ is determined by the injection of turbulent kinetic energy which is given by the surface flux. We use flux forms for the surface boundary conditions ($z = 0$) of $E$ and $\psi$ as follows:

$$F_E = K_E \frac{\partial E}{\partial z} = \eta u_\tau^3, \tag{15.93}$$

$$F_\psi = K_\psi \frac{\partial \psi}{\partial z} = -\frac{c_\mu (c_\mu^0)^p}{\sigma_\psi} (m\alpha + n) K^{m+\frac{1}{2}} L^{n+1} (z_0)^{(m+\frac{1}{2})\alpha + n}. \tag{15.94}$$

As explained in the previous section for Noh and Kim (1999) model, injection of turbulence kinetic energy may be made only through the open water in the presence of sea ice.

$$F_E = K_E \frac{\partial E}{\partial z} = \eta u_\tau^3 (1 - a), \tag{15.95}$$

where $a$ is sea ice area fraction.

The parameter $K$ can be determined from

$$K = \left( -\frac{\sigma_k^\psi}{c_\mu \alpha L} F_E \right)^{\frac{2}{3}} \frac{1}{z_0^\alpha}, \tag{15.96}$$

where (15.89), (15.92) and (15.93) are used.

At the bottom, the logarithmic boundary layers are assumed, in which $l = \kappa(z + H + z_{0b})$ is supposed. The bottom boundary conditions ($z = -H$) for $E$ and $\psi$ are given by flux forms as follows:

$$F_E = K_E \frac{\partial E}{\partial z} = 0, \tag{15.97}$$

$$F_\psi = K_\psi \frac{\partial \psi}{\partial z} = \frac{n (c_\mu^0)^{p+1} \kappa^{n+1}}{\sigma_\psi} E^{m+\frac{1}{2}} (z_{0b})^n, \tag{15.98}$$

where $z_{0b}$ is the bottom roughness, which is set to be $z_{0b} = 1\,\mathrm{m}$. Implementation of the bottom boundary condition is realistic as compared to the Mellor and Yamada scheme and the Noh and Kim scheme.

### 15.4.3 Model parameters

Umlauf and Burchard (2003) investigated the properties of the generic model in some fundamental flows and derived the constraints on the model parameters ($c_\mu^0$, $c_{\psi 1}$, $c_{\psi 2}$, $c_{\psi 3}$, $\sigma_k^\psi$, $\sigma_\psi$, $m$ and $n$). Table 15.5 is a recommended parameter set for the generic model by Umlauf and Burchard (2003), based on their calibration. MRI.COM uses this as the default parameters. Note that the parameter $p$ (the factor $(c_\mu^0)^p$ in (15.77)) is mathematically irrelevant, since (15.84) can be multiplied by any constant without changing the solution ($p = 2.0$ is used as the default value).

Table15.5 A recommended parameter set for the generic model by Umlauf and Burchard (2003), where $\kappa = 0.4$, $(c_\mu^0)^2 = 0.3$, and $c_{\psi 1} = m$ are assumed. The value of the parameter $c_{\psi 3}^-$ is based on the Algebraic Reynolds-Stress Model (ASM) of Canuto et al. (2001). In unstable situations ($P_\mathrm{b} > 0$), a different value of the parameter $c_{\psi 3}$ needs to be used. In MRI.COM, $c_{\psi 3}^+ = 1.0$ is adopted.

| $\alpha$ | $L$ | $m$ | $n$ | $\sigma_k^\psi$ | $\sigma_\psi$ | $c_{\psi 1}$ | $c_{\psi 2}$ | $c_{\psi 3}^-$ |
|---|---|---|---|---|---|---|---|---|
| −2.0 | 0.20 | 1.00 | −0.67 | 0.80 | 1.07 | 1.00 | 1.22 | 0.05 |

### 15.4.4 Stability functions

The version A of the Canuto et al. (2001) stability functions is expressed as follows:

$$\hat{c}_\mu = c_\mu (c_\mu^0)^3 = \frac{0.1070 + 0.01741\alpha_N - 0.00012\alpha_M}{1 + 0.2555\alpha_N + 0.02872\alpha_M + 0.008677\alpha_N^2 + 0.005222\alpha_N\alpha_M - 0.0000337\alpha_M^2}, \tag{15.99}$$

$$\hat{c}'_\mu = c'_\mu (c_\mu^0)^3 = \frac{0.1120 + 0.004519\alpha_N + 0.00088\alpha_M}{1 + 0.2555\alpha_N + 0.02872\alpha_M + 0.008677\alpha_N^2 + 0.005222\alpha_N\alpha_M - 0.0000337\alpha_M^2}, \tag{15.100}$$

where

$$\alpha_M = \frac{E^2}{\epsilon^2} M^2, \qquad \alpha_N = \frac{E^2}{\epsilon^2} N^2 \tag{15.101}$$

are nondimensional parameters referred to as the shear number and the buoyancy number. Using (15.79), they are related to the nondimensional parameter used by the Mellor and Yamada model (15.40) and (15.41) as

$$g_M = \frac{(c_\mu^0)^6}{2}\alpha_M, \quad g_H = \frac{(c_\mu^0)^6}{2}\alpha_N. \tag{15.102}$$

These are presented in Burchard and Bolding (2001)[‡]. MRI.COM adopts these as the stability functions for the Umlauf and Burchard (2003) model.

### 15.4.5 Implementation

Equations (15.83) and (15.84) are solved for the prognostic variable $E$ and $\psi$ in the subroutine `gls_main` in `gls.F90` as the last procedure of each time step. The forward finite difference is used in the time evolution. The implicit method is used for the vertical diffusion of the turbulent kinetic energy or generic variable and energy dissipation term, since these terms could become significantly large (see Section 23.5). The new $E$ and $\psi$ are used to determine the coefficients of viscosity and diffusivity for the next time step.

The turbulent kinetic energy and the master length scale are defined at the center of the tracer cell $(i, j, k - \frac{1}{2})$. The specific expression for the discretized form of the turbulent kinetic energy ($E$) equation is as follows:

$$\begin{aligned}\frac{E^{n+1}_{k-\frac{1}{2}} - E^n_{k-\frac{1}{2}}}{\Delta t} =& \frac{1}{\Delta z_{k-\frac{1}{2}}}\left[\frac{K_{E\,k-1}(E^{n+1}_{k-\frac{3}{2}} - E^{n+1}_{k-\frac{1}{2}})}{\Delta z_{k-1}} - \frac{K_{E\,k}(E^{n+1}_{k-\frac{1}{2}} - E^{n+1}_{k+\frac{1}{2}})}{\Delta z_k}\right] \\ &+ P_\mathrm{s} + P_\mathrm{b} - (c_\mu^0)^3 E^{n+1}_{k-\frac{1}{2}} (E^n_{k-\frac{1}{2}})^{\frac{1}{2}} / l^n_{k-\frac{1}{2}}.\end{aligned} \tag{15.103}$$

[‡] Note that definition of $c_\mu$ and $c'_\mu$ in Burchard and Bolding (2001) is different than that of this chapter. $\hat{c}_\mu$ and $\hat{c}'_\mu$ here correspond to $c_\mu$ and $c'_\mu$ of Burchard and Bolding (2001).

The specific expression for the discretized form of the generic variable ($\psi$) equation is as follows:

$$\frac{\psi^{n+1}_{k-\frac{1}{2}} - \psi^{n}_{k-\frac{1}{2}}}{\Delta t} = \frac{1}{\Delta z_{k-\frac{1}{2}}}\left[\frac{K_{\psi\,k-1}(\psi^{n+1}_{k-\frac{3}{2}} - \psi^{n+1}_{k-\frac{1}{2}})}{\Delta z_{k-1}} - \frac{K_{\psi\,k}(\psi^{n+1}_{k-\frac{1}{2}} - \psi^{n+1}_{k+\frac{1}{2}})}{\Delta z_{k}}\right] + \frac{\psi^{n}_{k-\frac{1}{2}}}{E^{n}_{k-\frac{1}{2}}}(c_{\psi 1}P_{\mathrm{s}} + c_{\psi 3}P_{\mathrm{b}}) - c_{\psi 2}(c^{0}_{\mu})^{3}\psi^{n+1}_{k-\frac{1}{2}}(E^{n}_{k-\frac{1}{2}})^{\frac{1}{2}}/l^{n}_{k-\frac{1}{2}}. \tag{15.104}$$

The shear and buoyancy production terms $P_{\mathrm{s}}$ and $P_{\mathrm{b}}$ are discretized as follows:

$$P_{\mathrm{s}} = \frac{1}{2}K_{M\,k-1}\frac{(u^{n+1}_{k-\frac{3}{2}} - u^{n+1}_{k-\frac{1}{2}})(u^{n+1}_{k-\frac{3}{2}} - u^{n}_{k-\frac{1}{2}})}{\Delta z_{k-1}\Delta z_{k-\frac{1}{2}}} + \frac{1}{2}K_{M\,k}\frac{(u^{n+1}_{k-\frac{1}{2}} - u^{n+1}_{k+\frac{1}{2}})(u^{n}_{k-\frac{1}{2}} - u^{n+1}_{k+\frac{1}{2}})}{\Delta z_{k}\Delta z_{k-\frac{1}{2}}} + \frac{1}{2}K_{M\,k-1}\frac{(v^{n+1}_{k-\frac{3}{2}} - v^{n+1}_{k-\frac{1}{2}})(v^{n+1}_{k-\frac{3}{2}} - v^{n}_{k-\frac{1}{2}})}{\Delta z_{k-1}\Delta z_{k-\frac{1}{2}}} + \frac{1}{2}K_{M\,k}\frac{(v^{n+1}_{k-\frac{1}{2}} - v^{n+1}_{k+\frac{1}{2}})(v^{n}_{k-\frac{1}{2}} - v^{n+1}_{k+\frac{1}{2}})}{\Delta z_{k}\Delta z_{k-\frac{1}{2}}}, \tag{15.105}$$

$$P_{\mathrm{b}} = -\frac{1}{2}K_{H\,k-1}\frac{B^{n+1}_{k-\frac{3}{2}} - B^{n+1}_{k-\frac{1}{2}}}{\Delta z_{k-1}} - \frac{1}{2}K_{H\,k}\frac{B^{n+1}_{k-\frac{1}{2}} - B^{n+1}_{k+\frac{1}{2}}}{\Delta z_{k}}. \tag{15.106}$$

The discrete expression for the shear production and the buoyancy production follows Burchard (2002), which is consistent with the conservation law of the sum of mean and turbulent energy.

To summarize, the numerical operations proceed in the following order:

1. Update the turbulent kinetic energy and generic variable using (15.103), (15.104), (15.105) and (15.106) under the boundary conditions, (15.93), (15.94), (15.97) and (15.98).
2. Diagnose the turbulent length scale using (15.78),
3. Calculate the vertical viscosity and diffusivity using (15.88) and (15.88) for the next time step.

### 15.4.6 Limiters

Some kind of limiters for the turbulent variables may be needed to ensure numerical stability. MRI.COM supposes the following conditions.

- Lower limiters of the turbulent kinetic energy and generic variable, $E_{\mathrm{min}}$, $\psi_{\mathrm{min}}$, are introduced as basic limiters.
- If one of $E$ and $\psi$ becomes less than the limiter, turbulence is considered as stagnant. That is,

$$E = E_{\mathrm{min}}, \quad \psi = \psi_{\mathrm{min}}, \quad l = l_{\mathrm{stag}}, \qquad \text{if either} \quad E \le E_{\mathrm{min}} \quad \text{or} \quad \psi \le \psi_{\mathrm{min}} \tag{15.107}$$

- When turbulence is stagnant, the diagnosed viscosity and diffusivity ($K_M$, $K_H$) should not exceed the background values ($K_{M\,\mathrm{bg}}$, $K_{H\,\mathrm{bg}} = 1.0 \times 10^{-6}\,\mathrm{m^2\,s^{-1}}$):

$$K_M = c_{\mu}(2E_{\mathrm{min}})^{1/2}l_{\mathrm{stag}} \le K_{M\,\mathrm{bg}}, \qquad K_H = c'_{\mu}(2E_{\mathrm{min}})^{1/2}l_{\mathrm{stag}} \le K_{H\,\mathrm{bg}} \tag{15.108}$$

- Stagnant value of the turbulent length-scale ($l_{\mathrm{stag}}$) is supposed to be the local vertical grid size ($\Delta z_{\mathrm{local}}$) for numerical stability.

Table15.6 Default limiters for GLS model in MRI.COM.

| $E_{\mathrm{min}}$ | $\psi_{\mathrm{min}}$ | $l_{\mathrm{stag}}$ |
|---|---|---|
| $\frac{1}{2}\left(\frac{10^{-6}}{0.1l_{\mathrm{stag}}}\right)^2$ | $(c^0_{\mu})^2\frac{E_{\mathrm{min}}}{l^{2/3}_{\mathrm{stag}}}$ | $\Delta z_{\mathrm{local}}$ |

### 15.4.7 Usage

Umlauf and Burchard (2003) model is invoked by `GLS` option on compilation.

Initial state for vertical diffusion of turbulence kinetic energy ($K_E$) and generic variable $K_\Psi$, turbulence kinetic energy ($E$), generic variable ($\Psi$), and length scale ($l$) is either read from restart file or set as the stagnant state defined in the

previous subsection. In the stagnant state, both of $K_E$ and $K_\Psi$ are set as $1 \times 10^{-6}\,\mathrm{m^2\,s}$. The initial state is specified by namelist `nml_gls_run`. Parameters are listed on Table 15.7.

Tuning parameters may be specified at run time by namelist `nml_gls`. Parameters are listed on Table 15.8.

Table15.7 namelist `nml_gls_run`

| variable name | units | description | usage |
|---|---|---|---|
| `l_rst_gls_in` | logical | `.true.` : Read restart files specified by `nmlrs_gls_`(`avk`, `avq`, `eke`, `psi`, `alo`) for the initial condition.<br>`.false.`: Start condition is that of no turbulence. See text for details. | default = `l_rst_in` of `nml_run_ini_state` |

Table15.8 namelist `nml_gls`

| variable name | units | description | usage |
|---|---|---|---|
| `mfnk` | 1 | $\eta$ of Eq. (15.93) | default = 100.0 |
| `l_wave_damp_seaice` | logical | Eq. (15.93) is used instead of (15.95) | default = `.false.` |

# Chapter 16

# Bottom Boundary Layer (BBL)

MRI.COM has an option of adopting a simple bottom boundary layer model (`BBL` option). This chapter describes the formulation and usage of this model.

## 16.1 General description

In general, neither dense overflows from the Nordic-Scotland-Greenland ridges to the Atlantic Ocean nor the dense downslope flows from the continental slope around Antarctica can be properly reproduced by $z$-coordinate models. The former becomes the core water of the North Atlantic Deep Water, and the latter becomes that of the Antarctic Bottom Water. As a result, the abyssal waters in the modeled ocean tend to exhibit a warming bias. To mitigate these deficiencies, MRI.COM incorporates a simple bottom boundary layer (BBL) model as introduced by Nakano and Suginohara (2002). In this model, BBL is attached immediately below the bottom of the interior oceanic domain and conceptually treated as a plane along the sea floor at the model's lowest vertical level (Figure 16.1). The following processes relevant to the overflow/downslope flows are (partly) incorporated into this BBL model:

- The advection along the bottom topography.
- The pressure gradient terms when the dense water lies on slope.
- The eddy activity to create the flow crossing $f/h$ contours.

## 16.2 Grid arrangement and exchanges

In $z$-coordinate models, the flow along the bottom topography is expressed as a sequence of horizontal and vertical movements along a staircase-like topography. When the number of vertical grid points representing the bottom topography is roughly the same as that of the horizontal grid points, the downslope flow can be reasonably represented even in $z$-coordinate models (Winton et al., 1998). In general, however, the number of the vertical grids used in ocean general circulation models is not large enough. Even if the number is large enough, the concentrations of tracers might be significantly diffused during their movement owing to the horizontal mixing with the surrounding waters. The incorporation of BBL remedies these problems.

The BBL grid cells in MRI.COM are arranged as in Figure 16.1. General interior grid cells in MRI.COM are composed of U-cells, but it is intuitively easier to understand the grid arrangement of BBL as if they are located at T-cells (represented by "•" points of Figure 16.1a and b). The T-cells in BBL are located just below the bottom of interior T-cells even if an interior T-cell consists of only one quarter of a U-cell (Figure 16.1b). The U-cells in BBL are regarded as slanting cells connecting neighboring T-points in BBL (Figure 16.1d).

For the purpose of calculating horizontal exchanges between BBL cells due to advection and subgrid-scale mixing, the *primary* BBL is attached below the normal ocean grid (Figures 16.1a and c). Assuming that the number of the vertical grids, `km`, is 50 before BBL option is applied, the number of vertical grids, `km`, becomes 51 (50 + 1) when BBL option is applied. In addition, to easily express the vertical exchange between the BBL cells and the inner ocean cells, we place a *dummy* BBL cell just below the bottom grid of each inner column and copy the temperature, salinity, and velocities from the primary BBL cell (Figures 16.1b and d).

Regarding vertical advection, primary vertical mass transport at the upper surface of BBL is defined at T-cell as in the interior (there is not vertical transport at the bottom of BBL). Even when the horizontal area of the bottom of the interior T-cell is smaller than that of BBL, all vertical mass transport at the top of BBL flows into or out of the bottom of the interior cell (Figure 16.1b and d). Tracers immediately above and below are carried by this vertical transport. In the same manner as explained in Chapter 6, the continuity equation for the U-cell is defined as an average of those of surrounding

T-cells (6.20). At each of the T-points connecting the bottom of the interior and the BBL, velocity (momentum) at all the U-cells in BBL that surround the T-point participates in the vertical momentum advection.

Regarding vertical mixing, tracer in BBL is exchanged with the one at the bottom of the interior as in vertical advection (the blue arrow in Figure 16.1b). On the other hand, velocity in BBL is exchanged with the one at the bottom of the water column of the same U-point (the blue arrow in Figure 16.1d), whose quarter cells may not necessarily constitute bottom T-cells that communicate with T-cells of the BBL.

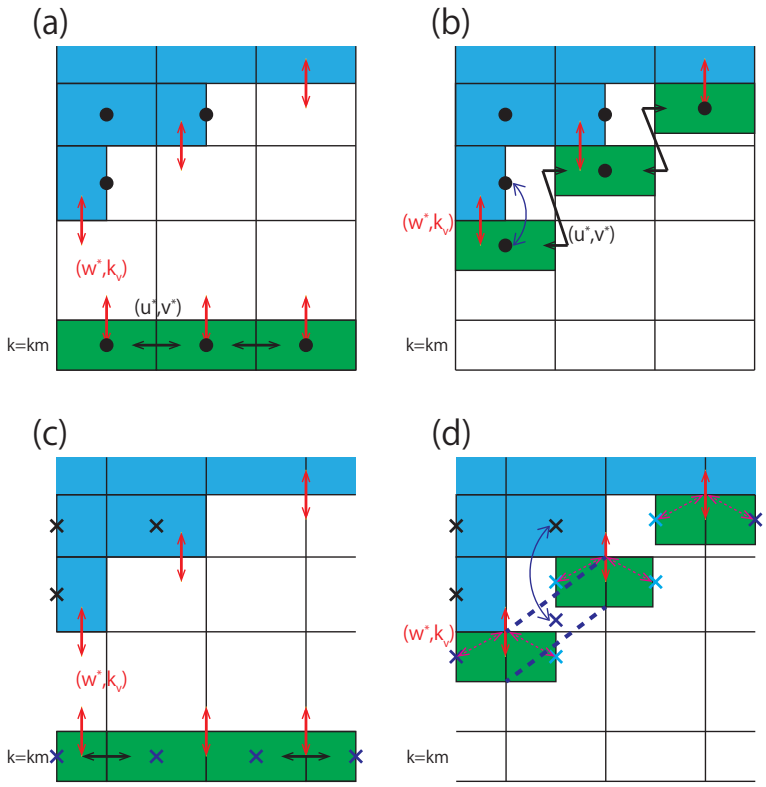


Figure16.1 Grid arrangement and schematic of horizontal and vertical exchange of tracers. (a, b) Arrangement of T-cell represented by "•" symbols. (c, d) Arrangement of U-cell represented by "×" symbols. The primary BBL cells lies at the bottom of the main (interior) oceanic domain (a and c). Horizontal advection and subgrid-scale mixing is computed there (solid black arrows). In relation to the interior, the T-cells in BBL are located just below the bottom of interior T-cells even when an interior T-cell consists of only one quarter of a U-cell (Figure 16.1b). The U-cells in BBL are regarded as slanting cells connecting neighboring T-points in BBL (dashed blue line in d). Vertical transport into and out of BBL occurs according to the primary vertical velocity defined at T-points (solid red arrows). Diagonally upward / downward advection of momentum may occur along the dashed red arrows in (d). Vertical mixing of tracers and momentum occurs between the cells indicated blue arrow in (b) and (d), respectively.

## 16.3 Pressure gradient terms

### a. Formulation

BBL of MRI.COM is attached at the bottom of interior T-cells. U-cells of BBL are regarded as slanting and connecting the surrounding T-points. (Figure 16.1d). In other words, sea floor is considered to have gradient along U-cells.

The pressure perturbation term in eq. (2.54) is

$$\begin{aligned}\frac{1}{\rho_0}\nabla_s p' &= \frac{1}{\rho_0}\nabla p'\big|_{s=-H(x,y)} - \frac{1}{\rho_0}\partial_s p'\nabla H(x,y)\\ &= \frac{1}{\rho_0}\nabla p'\big|_{s=-H(x,y)} + \frac{g\rho'}{\rho_0}z_s\nabla H(x,y),\end{aligned} \tag{16.1}$$

where $s$ means the depth coordinate along the sea floor. The geopotential term is

$$\frac{g\rho'}{\rho_0}\nabla_s z = \frac{g\rho'}{\rho_0}\nabla z\big|_{s=-H(x,y)} - \frac{g\rho'}{\rho_0}z_s\nabla H(x,y). \tag{16.2}$$

Then, the pressure gradient for a U-cell in BBL is expressed as

$$\frac{1}{\rho_0}\nabla_s p' + \frac{g\rho'}{\rho_0}\nabla_s z = \frac{1}{\rho_0}\nabla p'\Big|_{s=-H_{\mathrm{BBL}}(x,y)} + \frac{g\rho'}{\rho_0}\nabla z\Big|_{s=-H_{\mathrm{BBL}}(x,y)}. \tag{16.3}$$

b. Discretization

Horizontal gradient in (16.3) is evaluated along the bottom slope, not along the constant $s$-surface.

The depth of U-point in BBL ($z = z_{\mathrm{BBL}}$) that appears in the geopotential term is separated into time-independent ($-H_{\mathrm{BBL}}$) and time-dependent ($z'$) part, so that

$$\frac{g\rho'}{\rho_0}\nabla z\Big|_{s=-H_{\mathrm{BBL}}(x,y)} = -\frac{g\rho'}{\rho_0}\nabla H_{\mathrm{BBL}} + \frac{g\rho'}{\rho_0}\nabla z'\Big|_{s=-H_{\mathrm{BBL}}(x,y)}. \tag{16.4}$$

The pressure perturbation at T-point in BBL, whose vertical grid index is $k = ktbtm$, is computed by adding an increment due the downward vertical integration along the T-point from the corner of the upper face of the U-cell at the bottom of interior, whose vertical grid index is $k = kbtm - 1$, to the T-cell in BBL ($k = ktbtm$). The finite difference form is given as follows:

$$\Delta p'_{i,j,ktbtm} = \sum_{l=kbtm-1}^{ktbtm-1} (\rho')_{i,j,l+\frac{1}{2}}(\mathtt{dzt})_{i,j,l+\frac{1}{2}} + g(\rho')_{i,j,ktbtm+\frac{1}{2}}\frac{(\mathtt{dzt})_{i,j,ktbtm+\frac{1}{2}}}{2}. \tag{16.5}$$

The gradient of pressure perturbation is computed as

$$\begin{aligned}(\nabla p_{\mathrm{BBL}}{}')_{i+\frac{1}{2},j+\frac{1}{2}} =& (\nabla_r p')_{i+\frac{1}{2},j+\frac{1}{2},kbtm-1} + \hat{\mathbf{x}}\frac{\frac{\Delta p'_{i+1,j+1,ktbtm}+\Delta p'_{i+1,j,ktbtm}}{2} - \frac{\Delta p'_{i,j+1,ktbtm}+\Delta p'_{i,j,ktbtm}}{2}}{\Delta x_{i+\frac{1}{2},j+\frac{1}{2}}} \\ &+ \hat{\mathbf{y}}\frac{\frac{\Delta p'_{i+1,j+1,ktbtm}+\Delta p'_{i,j+1,ktbtm}}{2} - \frac{\Delta p'_{i+1,j,ktbtm}+\Delta p'_{i,j,ktbtm}}{2}}{\Delta y_{i+\frac{1}{2},j+\frac{1}{2}}}.\end{aligned} \tag{16.6}$$

The geopotential term is computed as

$$\begin{aligned}&\left[\frac{g\rho'}{\rho_0}\nabla z_{\mathrm{BBL}}\right]_{i+\frac{1}{2},j+\frac{1}{2}} \\ &= -\frac{g}{\rho_0}\left\{\left[\frac{\frac{\rho'_{i+1,j}+\rho'_{i,j}}{2}\frac{H_{\mathrm{BBL}i+1,j}-H_{\mathrm{BBL}i,j}}{\Delta x_{i+\frac{1}{2},j}} + \frac{\rho'_{i+1,j+1}+\rho'_{i,j+1}}{2}\frac{H_{\mathrm{BBL}i+1,j+1}-H_{\mathrm{BBL}i,j+1}}{\Delta x_{i+\frac{1}{2},j+1}}}{2}\hat{\mathbf{x}}\right]\right. \\ &\quad\left. + \left[\frac{\frac{\rho'_{i,j+1}+\rho'_{i,j}}{2}\frac{H_{\mathrm{BBL}i,j+1}-H_{\mathrm{BBL}i,j}}{\Delta y_{i,j+\frac{1}{2}}} + \frac{\rho'_{i+1,j+1}+\rho'_{i+1,j}}{2}\frac{H_{\mathrm{BBL}i+1,j+1}-H_{\mathrm{BBL}i+1,j}}{\Delta y_{i+1,j+\frac{1}{2}}}}{2}\hat{\mathbf{y}}\right]\right\} \\ &\quad + \frac{g}{\rho_0}\left\{\left[\frac{\frac{\rho'_{i+1,j}+\rho'_{i,j}}{2}\frac{z'_{i+1,j}-z'_{i,j}}{\Delta x_{i+\frac{1}{2},j}} + \frac{\rho'_{i+1,j+1}+\rho'_{i,j+1}}{2}\frac{z'_{i+1,j+1}-z'_{i,j+1}}{\Delta x_{i+\frac{1}{2},j+1}}}{2}\hat{\mathbf{x}}\right] + \left[\frac{\frac{\rho'_{i,j+1}+\rho'_{i,j}}{2}\frac{z'_{i,j+1}-z'_{i,j}}{\Delta y_{i,j+\frac{1}{2}}} + \frac{\rho'_{i+1,j+1}+\rho'_{i+1,j}}{2}\frac{z'_{i+1,j+1}-z'_{i+1,j}}{\Delta y_{i+1,j+\frac{1}{2}}}}{2}\hat{\mathbf{y}}\right]\right\}.\end{aligned} \tag{16.7}$$

In the source code, the depth of T-point `hot` is used for $H_{\mathrm{BBL}}$. To be exact, (`hot` − `dzt_cnst`/2) should be used. However, because the initial thickness of the BBL (`dzt_cnst`) is spatially uniform in MRI.COM, this omission would not affect the result.

## 16.4 Eddy effects

In the rotational frame, the dense water along the continental slope flows along $f/h$ without the eddy effects. In this case, introducing the BBL model does not lead to a better representation of the overflow/downslope-flow in the Nordic Seas or on the continental shelf around Antarctica.

In the real world, eddy effects create the cross $f/h$ flow, resulting in the overflow/downslope-flows. Jiang and Garwood (1996) investigated the three-dimensional features of downslope flows using an eddy-resolving model and demonstrated that the dense water descends roughly 45° left to the geostrophic contour (in the northern hemisphere) with vigorous eddy activity. The observation of significant eddy activity south of the Denmark Strait is consistent with this result. In order to

incorporate this effect into the non-eddy resolving models, we apply Rayleigh drag whose coefficient is nearly equal to the Coriolis parameter, $\alpha \simeq f$. In this case, the geostrophic balance is modified and written as follows:

$$-fv = -\frac{1}{\rho_0}\frac{\partial p}{\partial x} - \alpha u, \tag{16.8}$$

$$fu = -\frac{1}{\rho_0}\frac{\partial p}{\partial y} - \alpha v, \tag{16.9}$$

After some algebra we obtain

$$-f\left(v - \frac{\alpha}{f}u\right) = -fv' = -\frac{1}{\rho_0}\frac{\partial p}{\partial x}, \tag{16.10}$$

$$f\left(u + \frac{\alpha}{f}v\right) = fu' = -\frac{1}{\rho_0}\frac{\partial p}{\partial y}, \tag{16.11}$$

where $v' = v - (\alpha/f)u$ and $u' = u + (\alpha/f)v$ correspond to the geostrophic velocity for the pressure gradient. If we put $\alpha = f$, the direction of the flow is 45° to the right of the pressure gradient. In general, the horizontal pressure field is parallel to the topographic contour near the deep water formation area. Thus, incorporating the Rayleigh drag coefficient, $\alpha = f$, leads to the dense water descending 45° to the left of the geostrophic contour.

Because this Rayleigh drag is thought to be caused by the eddy activity and is observed where the dense water descends to the deep layer, the coefficient of the Rayleigh drag should be parameterized as a function of the local velocity and topography. However it is very difficult to appropriately determine this function in coarse-resolution models. Accordingly, in the default setting of BBL option in MRI.COM, the depth range where $\alpha = f$ is arbitrarily set above 2500 m in the northern Atlantic and above 4000 m around Antarctica to represent the observed dense overflow/downslope-flow. Below those depths, $\alpha$ is set to zero. This setting may be explicitly specified by using namelist `nml_bblrayfrc` (Table 16.1).

## 16.5 Usage

In this section, we show how to use the BBL model in the MRI.COM.

- Add `BBL` option in the file `configure.in`.
- Set the lowest layer of the array `dz(km)` as the thickness of BBL. Fifty to one hundred meters is recommended for the thickness of BBL, which roughly corresponds to the observed thickness of the BBL layer near the Denmark Strait.
- Append `ho4bbl`, `exnnbbl` to `file_topo` after `ho4`, `exnn` (Section 25.2.2), following `docs/README_Options.md`.
- Set the region where non-zero Rayleigh drag coefficient is applied (`nml_bblrayfrc`; Table 16.1). The default setting is above 2500 m in the North Atlantic and above 4000 m around the Southern Ocean.

If model integration starts from the 3-D distribution of temperature and salinity, the temperature and salinity in the BBL cells are set to those in the lowermost inner cells.

Example of `configure.in` with `BBL` option

```
OPTIONS="BBL"
IMUT=184
JMUT=171
KM=48
```

The file that contains topographic information is read by the model at run time as follows (see also Section 25.2.2).

How topography data (`file_topo`) with BBL is read by model

```
integer(4) :: ho4(imut,jmut),exnn(imut,jmut)
integer(4) :: ho4bbl(imut,jmut),exnnbbl(imut,jmut)
integer(4),parameter :: lun = 10
open(lun, file=file_topo, form=unformatted)
read(lun) ho4, exnn
read(lun) ho4bbl, exnnbbl ! This is for BBL.
```

Table16.1 Namelist `nml_bblrayfrc` for setting the lower limit above which Rayleigh damping is applied in BBL

| variable | units | description | usage |
|---|---|---|---|
| `deprfcn` | cm | subjective lower limit of depth (for northern hemisphere) above which Rayleigh damping is applied | default = 2500 m<br>= $2500 \times 10^2$ cm |
| `deprfcs` | cm | subjective lower limit of depth (for southern hemisphere) above which Rayleigh damping is applied | default = 4000 m<br>= $4000 \times 10^2$ cm |

## 16.6 Usage notes

### 16.6.1 Limit of the region where BBL model should be applied

Ideally, the BBL model should be applied universally and its behavior should change according to the local oceanic state. In the real configuration, the BBL model is only effective near the abyssal water formation areas. When used in other areas, such as the near the equator, the BBL model does not improve the tracer and velocity fields. Furthermore, because the BBL model connects the model cells along the topography, it inevitably induces a water mass exchange between the cold abyssal water and the warm shallow water. Thus, unphysical diapycnal diffusion could occur with the BBL model. This effect is not severe in high latitudes where the difference in temperature between the shallow continental shelves and the deep layer is expected to be small, but it is extremely problematic for the cells in low latitudes. This problem is similar to the problem for typical $\sigma$-layer models. To prevent this, it is recommended that the BBL model should be applied only to the regions where the processes reproduced by the BBL model are thought to be important.

### 16.6.2 Limits of the BBL

Linear interpolation of the temperature and salinity along an extremely steep slope may cause problems. For the default setting of MRI.COM, the BBL model is not applied in such places and isolated grids. This setting may be modified by using namelist `nml_bblgeo_limit` (Table 16.2).

Table16.2 Namelist `nml_bblgeo_limit` for limiting the range where BBL scheme is applied

| variable | units | description | usage |
|---|---|---|---|
| `hbblmin` | cm | for sea floor depth shallower than `hbbldmin`, BBL is not applied | default = 0 m |
| `bbldmax` | cm | if the sea floor is deeper than that of the neighboring point by `bbldmax`, the BBL is not applied | default = 10 000 m<br>$10\,000 \times 10^2$ cm |

### 16.6.3 Notes for program coding and analyses

In each vertical column, the BBL exists both at the bottom cell ($k$ = `km`) and at the lowest ocean cell ($k$ = `exn(i,j)`). In general, the lowest ocean cell of the T-point and U-point for the same horizontal indices might differ. Thus, the treatment of topographic mask array `atexl` and `aexl` is always very confusing. At the bottom cells ($k$ = `km`) that corresponds the primary BBL cells, we set `atexl` = 1 and `aexl` = 1 while we set `atexl` = 1 and `aexl` = 0 at the lowest ocean cells that corresponds the dummy BBL cells. In taking global average, the treatment of `atexl` = 1 in the BBL model needs special care to avoid double counting.